UNIVERSITY OF OKLAHOMA

GRADUATE COLLEGE

Multi-Material Extrusion Based Additive Manufacturing of Flexible Polymetric Materials

A THESIS

SUBMITTED TO THE GRADUATE FACULTY

in partial fulfillment of the requirements for

Degree of

MASTER OF SCIENCE

By

CONNOR LAWRENCE
Norman, Oklahoma
2024

Multi-Material Extrusion Based Additive Manufacturing of Flexible Polymetric Materials

A THESIS APPROVED FOR THE

SCHOOL OF AEROSPACE AND MECHANICAL ENGINEERING

BY THE COMMITTEE CONSISTING OF

Dr. Yingtao Liu, Chair

Dr. Chris Billings, Co-Chair

Dr. Yijie Jiang

© Copyright by CONNOR LAWRENCE 2024
All Rights Reserved.

Acknowledgements

I am immensely thankful to Dr. Yingtao Liu, serving as my thesis advisor, for his constant guidance, expertise, and support throughout the years. Additionally, I would like to thank all the students in his lab, for providing insight and feedback wherever possible. Thank you to Caylin Nimmo, for lending his constant expertise in the field of direct ink writing to me.

Additionally, thank you to Dr. Yijie Jiang for serving on my thesis committee, as well as allowing me to use the rheometer in his lab. Without your help, my characterization of the printing filament to improve my printing process would not be possible.

Thank you to all my friends and family, for providing continuous support over the years, and always believing in me. Your confidence in me has inspired me throughout my academic career, especially my time as a graduate student.

I would also like to thank Lane Taylor and Blake Herren for laying previous groundwork for direct ink writing at the University of Oklahoma, including modifying the pneumatic Ender 3 used for all print attempts. Without their efforts, this paper would not be possible.

Table of Contents

Table of Figures

Table of Tables

Abstract

Direct ink writing (DIW) is a 3D printing technique, capable of printing many different polymers that cannot be 3D printed using other methods. Previous DIW attempts at the University of Oklahoma using a modified Ender 3 printer, to pneumatically print material, focused on printing a carbon nanotube mixture into a silicon resin print bath. Attempts to replicate this process proved successful while simultaneously increasing familiarization with the process. Using direct ink writing material extrusion, a two-material circular nozzle designed to print multiple materials simultaneously was designed, analyzed, and tested at the University of Oklahoma. Additionally, conceptual designs for other nozzles to print from two to five materials at once were also created. A Photon Mono M5s resin printer could create the desired geometry of the nozzle. Provided that the filament utilized was capable of being 3D printed, with a high enough viscosity and shear-thinning properties, the nozzle could create complex two-dimensional geometry. This complex geometry utilized print times of almost 10 minutes with no adjustments to printing pressure necessary mid-print. Additionally, material extrusion could be stopped and restarted with no issues. Future efforts could serve to test out the mechanical properties of pneumatically extruded materials in comparison to the material properties, while also creating three-dimensional geometry or testing different materials in each side of the nozzle.

Chapter 1: Introduction

1.1: Eco-Flex 00-30 Overview

Wearable sensors represent a rapidly expanding field in technology, primarily aimed at enhancing personal health monitoring and integrating seamlessly with everyday life [1-3]. These devices are designed to be worn on the body, often incorporated into clothing or accessories, to continuously monitor a range of physiological and environmental parameters. The materials used in developing wearable sensors are crucial for their functionality and user comfort. Common materials include flexible polymers, conductive textiles, and silicone-based substrates, which offer durability and stretchability essential for body movements [4-6]. Recent advancements also involve integrating nanoparticles and nanofibers in flexible polymers as nanocomposite materials, which improve the sensor's sensitivity and accuracy [7-10]. These materials are chosen not only for their physical and electronic properties but also for their compatibility with human skin and ability to function reliably in various environmental conditions.

Flexible silicone rubbers, such as polydimethylsiloxane (PDMS), or Eco-Flex 00-30 are materials commonly used in wearable sensor applications, as they are both flexible and durable, with Eco-Flex 00-30 able to stretch up to 900% at break [11, 12]. PDMS has a much higher Young's modulus value (between 0.4 MPa – 3.5 MPa), compared to Eco-Flex 00-30, which has a Young's modulus value between 100 kPa and 125 kPa [12]. Eco-Flex 00-30, sold by Smooth-On Materials, is a material commonly used as a matrix material in these wearable composites. It can also be used for anti-impact composites, as well as many different applications in the biomedical field, with

things such as prosthetic limbs, cushioning, synthetic vascular grafts, and sensors [13, 14]. The high stretchability and durability of the material help provide mechanical properties that can resemble biological tissues such as human skin [14]. Eco-Flex 00-30 can be extruded using the direct ink writing method of 3D printing. It is a thermoset material, as two chemicals, Eco-Flex 00-30 Platinum Cure Silicon Rubber Part A and Eco-Flex 00-30 Platinum Cure Silicon Rubber Part B are combined to create the silicon rubber gel, which then cures into silicon rubber. Eco-Flex 00-30 has a pot life, or work time, of 45 minutes and a cure time of 4 hours [11].

There are two main groups that polymers can be divided into: thermoplastics and thermosets. Thermoplastics soften when heated and become more and more fluid as heat is applied. The process of setting and curing the material is completely reversible, and since no chemical bonding occurs, they can be returned to their original liquid form before curing occurs. Thermoplastics generally offer high strength, shrink resistance, and easy bendability. Additionally, they are highly recyclable, with remolding/reshaping capabilities, making them an ideal choice in eco-friendly manufacturing over thermosets. The curing of thermoset materials is generally an irreversible process. Thermosets contain polymers that cross-link throughout the curing process, creating a chemical bond that is not reversible. As such, the risk of the material remelting to its original state when heat is applied is eliminated. Some benefits of thermosets are increased chemical resistance, heat resistance, and structural integrity. Additionally, they are cost-effective, but on the other hand, cannot be recycled like thermoplastics [15]. Since Eco-Flex 00-30 is a thermoset material, the reaction is not reversible, as it is a chemical reaction that occurs between the Part A and Part B chemicals to create silicon

rubber. As the material cures, during the 4 hour long curing process, cross-links are formed between the Part A and Part B chemicals, resulting in an irreversible chemical reaction, curing the material [11]. Eco-Flex 00-30 can be manufactured by using a mold or 3D printing and allowing it to cure either at room temperature or at a higher temperature [16, 17].

1.2: Additive Manufacturing Overview

Additive manufacturing is a relatively new manufacturing technique that, in contrast to traditional subtractive manufacturing, seeks to add material instead of removing it to create the desired geometry. Traditional additive manufacturing is based upon a horizontal layered approach, adding materials in slices that build up to create a full three-dimensional part [18]. According to the International Organization for Standardization (ISO)/American Society for Testing and Materials (ASTM), there are 7 different categories of additive manufacturing: binder jetting, directed energy deposition, material extrusion, material jetting, powder bed fusion, sheet lamination, and vat photopolymerization. Traditional 3D printing using polylactic acid (PLA), is considered fused deposition modeling, falling under the material extrusion category [19]. The two main categories of additive manufacturing focused on in this paper are material jetting, with the direct ink writing process, and vat photopolymerization, with a photopolymer used to create the geometry of the nozzle printed.

In material jetting, droplets of build material are deposited. Direct ink writing and 3D inkjet technology are both examples of this technology. Material jetting can be highly accurate in droplet deposition while also resulting in low waste and being good

for multiple material parts. However, support material is often required, with mainly photopolymers and thermoset resins able to be used [19].

With vat photopolymerization, the liquid polymer in a vat is cured by exposure to ultraviolet light, usually a wavelength of 405 nanometers. Stereolithography (SLA) and digital light processing (DLP) are two examples of this technology. Vat photopolymerization is good for large parts, providing very good accuracy and an excellent surface finish and details. However, it is limited to photopolymers, which can have a low shelf life and poor mechanical properties. It can also have a slow build process [19].

Direct ink writing is a method of additive manufacturing that can be used to print almost any viscous liquid. Like other 3D printing methods, DIW is the deposition of material layer-by-layer. It consists of using a nozzle to pneumatically push “ink” through a nozzle, with three-dimensional control over the extrusion location of the ink. Almost any viscous liquid can be printed, provided it can be extruded as a continuous filament, flowing smoothly without clogging the nozzle, and rapidly solidifying to maintain the geometry extruded. Direct ink writing extrusion can be placed into two groups: droplet, and continuous ink extrusion [20]. This paper will focus on the continuous ink extrusion part of DIW, with droplet extrusion not explored.

DIW can print various polymers, including synthetic, biopolymers, and composites. Other technologies, such as selective laser sintering, stereolithography, and fused filament fabrication, require specific types of polymers to print, meaning the method is limited to only a set group of polymers, whereas DIW is not, as melting,

sintering, or additional binding is not required before deposition. Many printing devices that print multiple materials simultaneously utilize DIW for material deposition [20].

With direct ink writing, the user has a few different variables that they have control over, including but not limited to nozzle diameter, print speed, and printing pressure. Using a nozzle with a smaller diameter can enhance the resolution of the print, but as a drawback, it requires higher extrusion pressure and more build time to avoid nozzle clogging. Likewise, a lower printing speed can give better print quality in terms of tolerances and fidelity but increases the time. With DIW, after extrusion, the ink must rapidly solidify to maintain its shape. When the ink is deposited, it is not at its final location; the ink ends up being "pulled" by the nozzle due to the continuous nature of the filament. Additionally, to be possible for DIW, the ink must be able to flow smoothly without discontinuity and not clog the nozzle with particles [20].

The advent of DIW has widely expanded the field of materials that are able to be 3D printed. It has greatly expanded the potential of manufacturing, as well as material engineering and design [20].

1.3: Previous Direct Ink Writing at the University of Oklahoma

Previous DIW work at the University of Oklahoma focused on printing a carbon nanotube, Eco-Flex 00-30 mixture into a silicon rubber resin bath to create wearable sensor technology. The created sensors had a low elastic modulus of 83.4 kPa, and a 535% maximum tensile strain before fracture, creating ultra stretchable sensors with high durability and sensitivity. Additionally, the carbon nanotubes provide piezoresistive sensitivity. Different nozzle diameters and printing pressures were tested, with the 1.5 wt% CNT ink being printable in nozzle diameters ranging from 0.2 mm to

0.61 mm, and printing pressures ranging from 138 kPa to 414 kPa. Electrical resistances of printed strain sensors were also measured, with 1.5, 2, and 2.5 wt% CNT loadings tested. The resistivity of both the ink and the resistance of the sensors decreased as CNT weight percentage increased due to a greater number of conductive networks. Additionally, the piezoresistive signals show a peak in resistance at the maximum strain of each cycle placed upon the sensors. Curing temperature and nozzle diameter were varied to find the parameters that produced the highest sensitivity sensor, with a 0.41 mm nozzle and a 150-degree Celsius curing temperature producing best results [12]. All print attempts for this paper utilized the same modified Ender 3 printer utilized for further print attempts in Chapter 2 and Chapter 4.

1.4: Multi-Material 3D Printing Review

One of the current leading research groups in the field of multi-material DIW is Jennifer Lewis's group at Harvard. Their research allows for the switching of materials within a nozzle using high frequency solenoids. Each printhead is capable of printing 8 different materials, each of which is held within their own chamber before the channels meet into a single channel that flows into the nozzle head. Using pneumatic extrusion, Lewis's group was able to achieve a theoretical value of 50 Hz for the frequency of material switching. However, the nozzle geometry to withstand the pressure is important, as well as eliminating upstream flows, resulting in the mixing of materials within the nozzle. The designed print head was capable of rastering a continuous fiber with a diameter of 250 microns. When the material was switched, at the transition time with a 90%/10% split between two materials, the diameter was observed to be approximately 320 microns, meaning that it enlarges when the material is switched.

However, this diameter, with a print speed of 20 mm/s, represents a frequency of approximately 60 Hz, greater than the theoretical 50 Hz. Lewis's group also printed an origami structure, with materials with vastly different material properties. The materials had Young's modulus values ranging from 0.61 to 3.92 GPa, proving that the print was successful with materials with vastly different mechanical properties [21].

Xu et al. also explored using DIW for metallic structures with removable supports. Metallic particles are mixed into the polymer, creating a metal-polymer material. Current DIW work using metal-polymer materials is unable to create large overhangs because a post-deposition thermal treatment is required to pyrolyze the polymer, as well as to sinter the metal particles. If supports are removed before the polymer is pyrolyzed, the overhang will collapse. If supports are not removed before the polymer is pyrolyzed, the supports will become fused to the rest of the structure and become inseparable after the thermal treatment. Xu et al. sought to use a different metal-polymer mixture or a ceramic-polymer mixture, such as copper or alumina, to create supports for a steel structure. Multiple different nozzles on the print head, placed side by side, extruded the material, with syringes connected to each material housing each individual metal-polymer or ceramic-polymer mixture. The copper supports led to no negative effects on the building structure of the steel and improved the electrical conductivity by 4 times, as well as the stiffness by 34%. The alumina supported lowered the stiffness of the building structure by 17%, but also did not contaminate the structure. Using multi-material printing, the geometry that was able to be created for DIW metallic 3D structures was broadened [22].

Jennifer Lewis's group also experimented with multi-material, multi-nozzle direct ink writing of soft materials. Using an ink composed of triblock copolymer, gelatin, and photopolymerizable polyacrylate materials, Lewis's group was able to successfully extrude this material out of nozzles to create complex geometry. However, their methodology utilized 16 nozzles, with 2 rows of 8 placed side-by-side, spaced 2.5 millimeters apart. Solenoids were used to control the ink flow and extruded pneumatically, giving the nozzles stop/start capabilities. The printing setup used by Lewis's group used a profilometer to scan a region of interest at regular intervals, collecting 800 data points in the direction of printing. Using this scan of the region of interest, they could alter the Z-height of the nozzles during printing, allowing for complex prints to be printed on regions with topographical differences [23].

1.5: Thesis Outline

This thesis is intended to discuss the evolution of the pneumatic printer to its present state, characterize the material printed, as well as providing analysis on the designed nozzles. Chapter 2 will focus on previous DIW attempts, writing G-code, utilizing the printer, as well as some attempts at creating three-dimensional geometry. Chapter 3 will discuss the nozzles designed for multi-material printing, as well as the analysis of them. Chapter 4 will focus on the results of print iterations utilizing these nozzles and the geometries printed. It will also include a rheological study of the printed material as well as a computational fluid dynamics (CFD) analysis of the nozzle. Chapter 5 will be a conclusion that also discusses future work and next steps, along with recommendations for improving the process.

Chapter 2: Direct Ink Writing Attempts

2.1: Printing Process Overview

The printer utilized to perform these direct ink writing prints is a modified Ender 3, modified to extrude material pneumatically at room temperature. The printer runs using Marlin G-code, with the numerical control of the print head using the same commands. To control the pneumatic valves of the printer, the hot end and the cooling fan commands are used to manipulate the solenoid. The command “M104 S200”, which sets the hot end temperature to 200 degrees Celsius, now opens the left pneumatic valve. The command “M104 S0”, setting the hot end temperature to 0 degrees Celsius, is used to close it. Likewise, the command “M106”, which traditionally is used to turn the cooling fan on, now opens the right valve, with “M107”, normally turning off the cooling fan, closing the right valve. The coordinate system of the modified Ender 3 is the same as a traditional Ender 3, with the X, Y, and Z coordinates used to refer to print geometry throughout the rest of the paper. Figure 1 below shows the coordinate system of the printer, with positive Z being in the upwards direction.

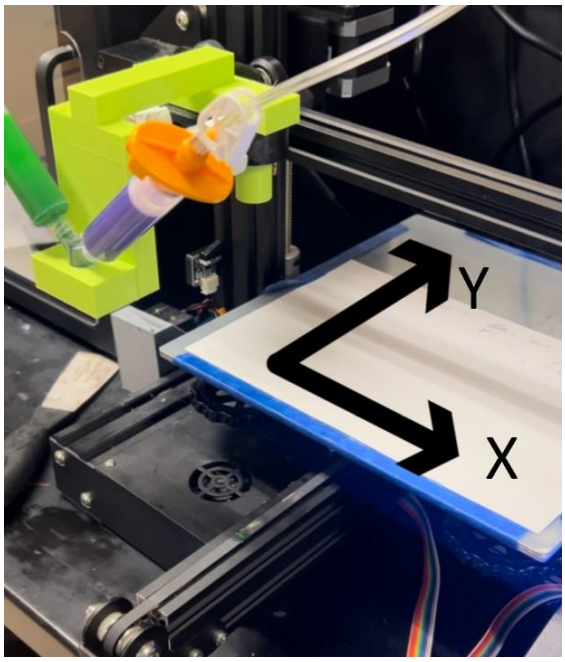

Figure 1: Coordinate System of the Modified Ender 3 Printer

The prints of the carbon fiber nanotube mixture were conducted within a resin bath mixture, consisting of a bottom layer and a top layer, meaning three total chemical mixtures had to be prepared for each print attempt. Table 1 below summarizes the formulas for these mixtures. The masses listed are based upon a 10-gram mixture of Eco-Flex 00-30, as 10 grams were mixed each time that the mixture was created. Eco-Flex 00-30 Part A Platinum Cure Silicone Rubber, Eco-Flex 00-30 Part B Platinum Cure Silicone Rubber, THI-VEX, SLO-JO Platinum Silicone Cure Retarder, and Silicone Thinner were all purchased from Smooth-On materials and used following manufacturer instruction. The carbon nanotubes described were 50-90 nm diameter, >95% carbon basis multiwalled carbon nanotubes purchased from Sigma-Aldrich.

Table 1: Mass Formulas for the Mixtures Used Based Upon 10 Grams of Eco-Flex 00-30

Chemical	Bottom Resin Bath Mixture	Top Resin Bath Mixture	Printing Filament Mixture
Eco-Flex 00-30 Part A	5 grams	5 grams	2.5 grams
Eco-Flex 00-30 Part B	5 grams	5 grams	2.5 grams
THI-VEX	0.05 grams	-	-
SLO-JO	0.2 grams	0.2 grams	-
Silicone Thinner	-	1 gram	-
Carbon Nanotubes	-	-	0.05 grams

The resin bath to print the filament in was first described by Muth et al. They discuss a form of "embedded 3D printing", or e-3DP, in which a viscoelastic ink is deposited into an elastomeric reservoir. Their elastomeric reservoir contains two elements: a filler fluid, and a reservoir. The reservoir material is a thicker, more viscous material with the goal of holding the filament in place. The filler material is a thinner, less viscous material that seeks to fill in the void space left in the elastomeric reservoir as the nozzle translates through it. Muth et al list a few criteria for the supporting reservoir and filler fluid for embedded 3D printing. The reservoir must support the creation of the geometry without the breakup of the ink filament, and the gaps in the reservoir must be quickly filled by the filler fluid. Additionally, the reservoir must be capable of curing into one solid elastic, stretchable material [24]. Through the usage of e3DP, Blake Herren was able to successfully print highly flexible nanocomposite sensors with piezoresistive capabilities [12]. This elastomeric reservoir, or resin bath, holds the

ink filament in place after printing, and allows the ink to take its time to cure following printing as the geometry is fully supported and held in place by the resin bath. Thus, ink filaments with longer curing times are capable of being printed through this method. The Smooth-On website states that the cure time for Eco-Flex 00-30 is approximately 4 hours, however, it was found experimentally that the resin bath for e3DP takes approximately 24 hours to cure [11]. One method discovered to speed up this process was leaving prints on the modified Ender 3 bed overnight with the bed at 60 degrees Celsius, allowing them to quickly cure in approximately 8 hours.

When creating the mixture for the bottom layer of the resin bath, the chemicals, with the appropriate masses displayed in Table 1 above, were added to an IntelliSpense 10cc Clear Pneumatic Syringe Barrel with a Gejoy luer lock needle tip cap on the end using a disposable syringe and nozzle. The mixture was measured on a B303 balance created by Mettler Toledo, capable of measurement to the thousandth of a gram. First, the 5 grams of Part A was added followed by 5 grams of Part B, again with a disposable syringe and nozzle. Then, in the same manner as the previous chemicals, 0.05 grams of THI-VEX was added, followed by 0.2 grams of SLO-JO. Following this, a 10cc white wiper piston by IntelliSpense was added to cover the top of the syringe barrel, and a Luer Lock Female-to-Female Polypropylene Syringe Adapter, manufactured by Dispense All, was placed on the tip of the syringe barrel after removing the Gejoy needle cap. The mixture was then mixed using another 10cc syringe and a plunger to push the mixture between the syringe barrels. This resulted in partially mixing up the mixture, preparing it to create a fully homogeneous mixture in the centrifuge. Following this, the syringe barrel containing the mixture was placed in an AR-100 centrifuge, by Thinky

Corporation, and mixed for 5 minutes, with a 2.5-minute deaeration period to ensure a homogenous mixture free of trapped gasses. An image of the printing bed is shown below in Figure 2. It is a disposable plastic bed, with a square printing bed approximately 40 millimeters by 40 millimeters at the bottom.

Figure 2: Print Bed Used for Carbon Nanotube DIW Attempts

The bottom layer of the resin bath was then extruded into the printing bed, with care taken to ensure that no bubbles formed within the resin. It was allowed to sit for approximately 5 minutes while the top layer of the resin bath was mixed within the centrifuge. The top layer of the resin bath was created in the same manner as the bottom layer of the resin bath, following the same process, except for with a slightly different chemical combination. For the top layer of the resin bath, Part A was initially added,

followed by Part B, then SLO-JO, and finally the silicon thinner. Once the top layer of the resin bath was homogenously mixed in the centrifuge, it was also placed into the printing bed, with care taken to ensure that no bubbles formed within the resin. Each 10cc syringe barrel of the resin bath could create enough of a resin bath for approximately 2 print beds each.

The filament for printing was created in a similar process as the bottom and top of the resin bath, using the correct chemical composition outlined in Table 1 above. A large laboratory spoon/spatula was used to load the carbon nanotubes into the syringe barrel. Only 5 grams of filament were mixed, compared to 10 grams of the top/bottom of the resin bath, as none of the print attempts used remotely close to 5 grams of filament. Additionally, since the carbon nanotubes are very lightweight, 10 grams of filament may not be capable of volumetrically fitting within the syringe barrel.

A 22-gauge nozzle was used to extrude the filament from the syringe barrel during printing. An image of the printing setup is shown in Figure 3 below. Approximately 20-25 psi was used to extrude the filament during printing, however, this pressure was continuously adjusted during the printing process. The Z-height of the print itself was set to 0.5 millimeters, however, as the print occurs within a resin bath, this value is trivial as long as the Z-height is greater than 0 and located within the resin bath. While printing, the printing speed was kept constant, and the printing pressure was actively tuned during the print. The filament was evaluated visually while printing on whether the thickness of the filament was too thick or too thin, with the printing pressure being adjusted accordingly. This was based off previous DIW experience with

the printer, with the correct pressure adjustments improving over time. The G-code was ran using Marlin firmware, using a microSD card, just like a normal Ender 3 printer.

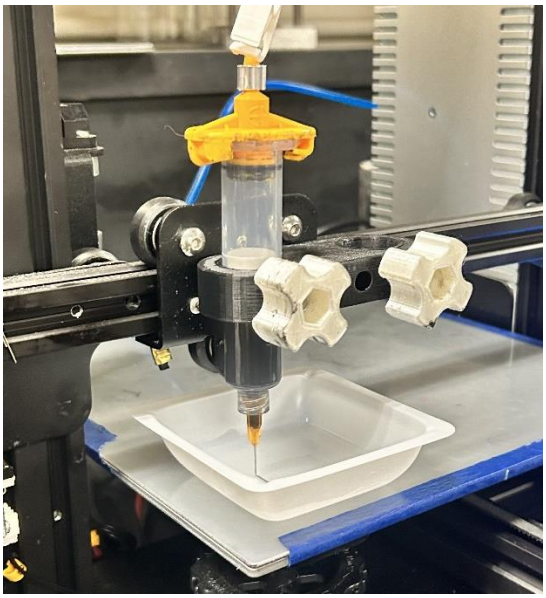

Figure 3: Image of the Carbon Nanotube Printing Setup

2.2: Two-Dimensional with Basic Geometry

The first shape tested using the printing process outlined in Chapter 2.1 above was a two-dimensional square, with side lengths of approximately 10 millimeters by 10 millimeters. To create this geometry, it was first modeled in SolidWorks, with the lines of the filament being 0.8mm wide and 0.8mm tall. Then, using Prusa Slicer, the geometry was sliced, creating the G-code. However, due to the configuration of the printer, the G-code needed to be modified to use the M104 commands to open and close the left nozzle. Using this same process, the G-code was modified for future print attempts, including three-dimensional geometry. Figures 4 and 5 below show examples of print results.

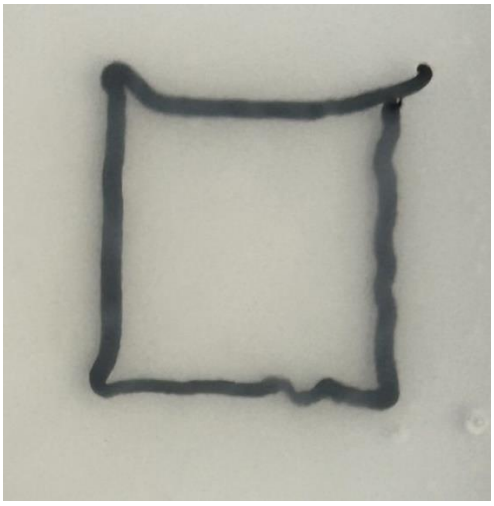

Figure 4: Square Print Attempt with Too High of Pressure

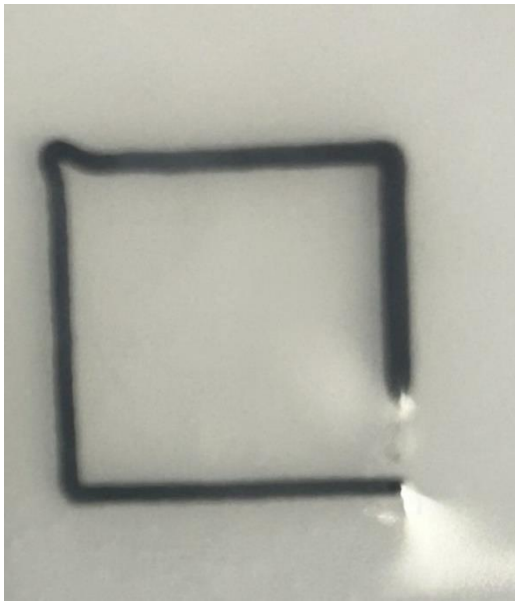

Figure 5: Square Print Attempt with Correct Pressure Level

Figure 4 above shows a print attempt with too high of a pressure, as can be seen due to the buckling filament. This occurs because too much filament is being extruded per unit of distance that the print head travels. On the other hand, the square in Figure 5 above shows a print attempt with correct pressure throughout most of the print attempt.

The print starts in the bottom right corner and moves counterclockwise. The second half of the square printed shows thick, straight lines, with corners of approximately 90 degrees. It should be noted that there were issues with the upper left corner, likely due to printing pressure being too high in that corner. Additionally, the pressure initially was too low when the print began, with no filament being extruded for a part of the first line of the square printed.

2.3: Two-Dimensional with Complex Geometry

To create the G-code for the more complex geometry, the same process was repeated as before. A star with a print area of approximately 31 millimeters by 31 millimeters was printed out. This was selected because the corners of the star are 36 degrees each, and the acute angle means that at the tip of the corner, the filament must wrap back in on itself. This geometry provides a challenge to create. Since the filament wraps back in on itself, there is too much material extruded, and thus a lower pressure or higher feed rate is necessary to maintain the same thickness of the material.

Figures 6-8 below show print results for the star G-code using the carbon nanotube filament. The printing pressure and printing speed can both be manipulated, as well as the time since the filament was mixed. To keep the variables consistent throughout the process, the printing speed was fixed at 30 millimeters per second for all print attempts, and the prints were immediately begun once the filament was done mixing in the centrifuge. This ensured that the only variable that could be manipulated was printing pressure during the printing process. The pressure required varied for each print, but usually fell between 20 and 25 psi, with slight tuning needed at the start of each print. However, once an ideal pressure was found, this was able to be used for the rest of the print with minimal tuning necessary. Figure 6 below is an example of the

printing pressure being too high. As seen in the straight lines of the star, they are wavy, which means that too much filament has been extruded. This could also be fixed by increasing the printing speed, but the printing speed was maintained at a consistent rate throughout the printing process. In contrast, Figure 7 below is an example of the printing pressure being too low. There is not enough filament extruded, as seen by the gaps in the straight lines of the star. Figure 8 below is an example of a good print, with thick filament lines. The filament lines are straight, unlike in Figure 6, and the lines are thick, with enough material extruded, unlike Figure 7. Figure 8 is a good example of a successful DIW print using this embedded 3D printing method. As the issues with this geometry were related to either printing pressure being too high or too low, these issues were the same as those previously seen in Chapter 2.2.

Figure 6: Star Print Attempt with Too High Pressure

Figure 7: Star Print Attempt with Too Low Pressure

Figure 8: Star Print Attempt with Correct Pressure

2.4: Three-Dimensional with Basic Geometry

For initial prints to look at the three-dimensional capabilities, two of the same squares described in Chapter 2.2 were printed, with one 1.5 millimeters in Z height above the other. The resin bath was cut using a razor blade following curing to take better images and visualize the prints better. Figure 9 below shows the prints from the side, with the bottom print always being in the upwards direction of the image. Figure 10 shows the print attempts, looking at the bottom print. The prints on the bottom usually had more accurate geometry than the prints on the top. As seen in the lower left print of Figure 9, there were issues with one of the corners increasing in Z-height while printed. Additionally, as seen in Figure 10 below, a lot of the corners of the squares tended to be rounded, likely due to the filament being "pulled" by the nozzle, discussed earlier in Chapter 1.2.

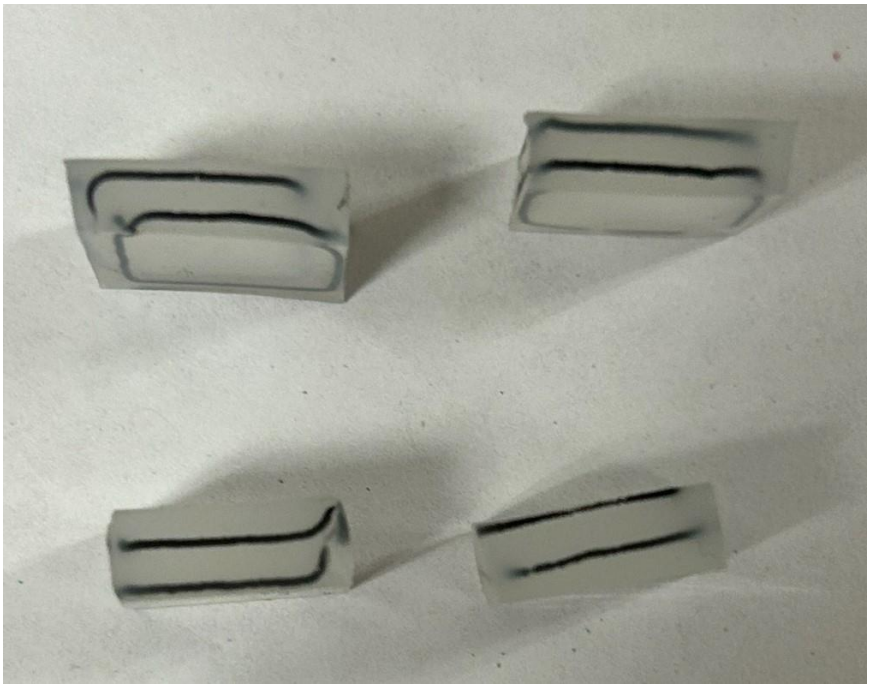

Figure 9: Two Squares Print, Image 1

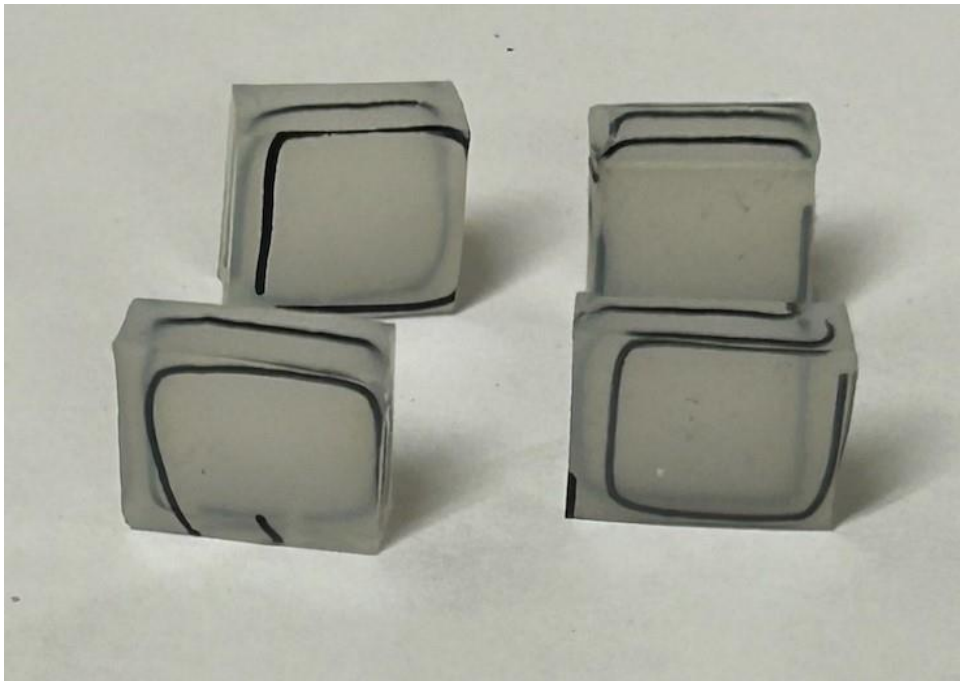

Figure 10: Two Squares Print, Image 2

2.5: Three-Dimensional with Complex Geometry

To test out the three-dimensional capabilities of this DIW process, a G-code was created that printed two of the same stars as described and printed in Chapter 2.3, with one star 1.5 millimeters in Z height above the other. The geometry of the star was the exact same, with the G-code being created by simply copying the code for one iteration of the star into the file and increasing the Z height, to print one star directly on top of the other.

As in Chapter 2.4, the resin bath was cut using a razor blade to better visualize and take images of the three-dimensional geometry of the prints. Figure 11 below shows the bottom of the print, with the bottom star printed visible, with Figures 12 and 13 showing the upper surface of the print, with the top star printed visible. As can be seen,

the bottom star turned out very well, however, the top stars had issues with filament being continuously extruded. Additionally, the corners of the stars would often buckle upwards, increasing in Z-height. As in Chapter 2.4, the bottom print consistently resembled the ideal geometry more often than the top print.

Figure 11: Image Showing Geometry of the Bottom Star

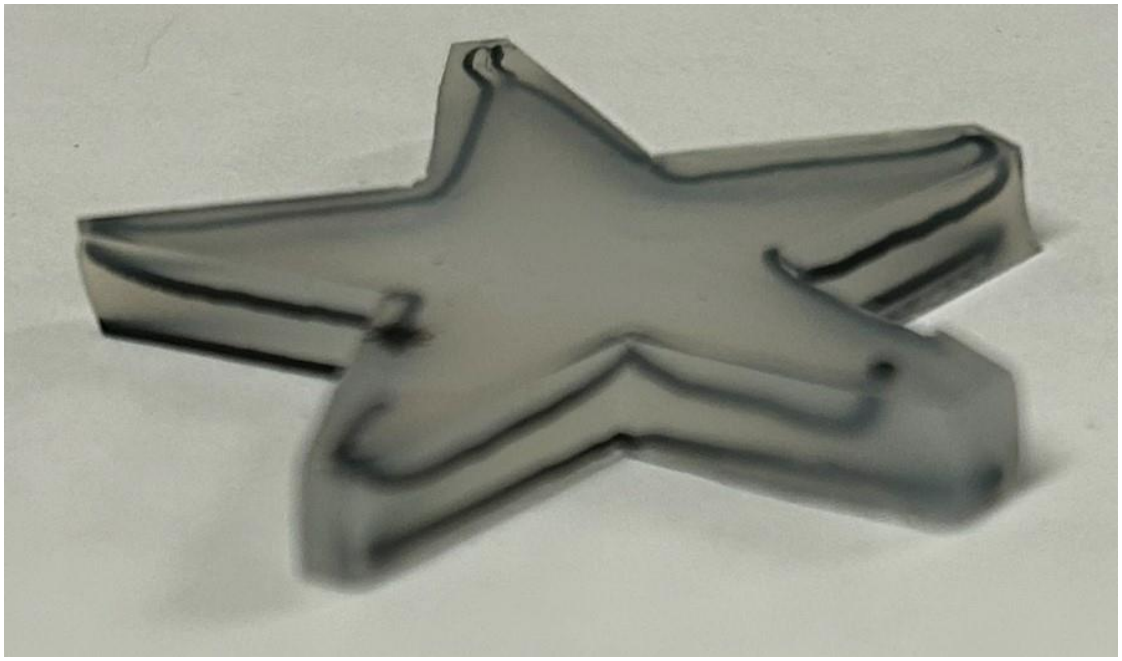

Figure 12: Print Attempt 1 of Three-Dimensional Stars

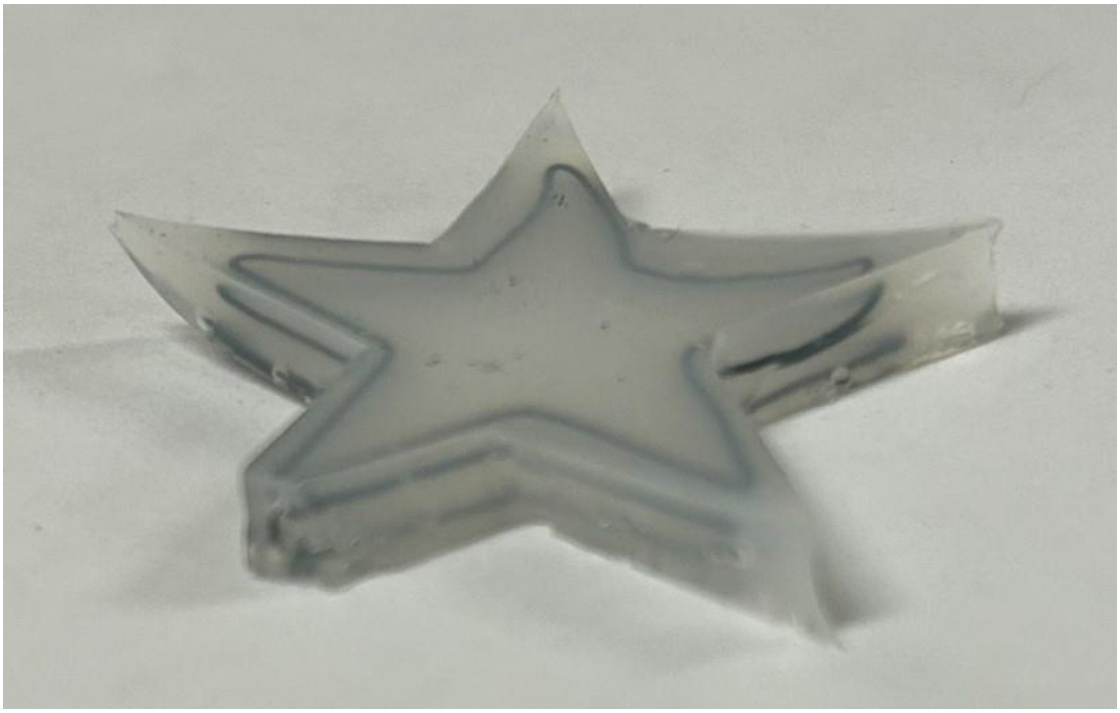

Figure 13: Print Attempt 2 of Three-Dimensional Stars

Chapter 3: Nozzle Designs/Analysis

3.1: Two Material Nozzle Design

For the design of the two-material nozzle, a few basic design constraints were taken into consideration. Firstly, it must be easily manufacturable, because it is not able to be tested if it is not able to be procured cheaply. Resin printing was the manufacturing method of choice due to the ability to hit tight tolerances to create complicated geometry, and the ease of operation of the resin printer. Additionally, mass manufacturing is simple using the resin printer. It also must be lightweight, as the nozzle, nozzle holder, and syringes with filament must fit on and be controlled by the stepper motors of an Ender 3 printer. Like other printers, it must come to a point at the tip of the nozzle where material is extruded to have the capability to create detailed geometry. A 22-gauge nozzle was the primary inspiration for the initial nozzle tip size, as this was the nozzle gauge size used for the previous printing attempts using the carbon nanotube filament. Additionally, it must be capable of printing two different materials at once, either concentrically or side by side. The chosen method for the two-material nozzle was side by side, as this geometry was simpler to manufacture and test with. Other nozzles were designed that were capable of printing multiple materials concentrically, however, they were not analyzed, or manufactured and tested. Two luer lock, 10cc syringe barrels must be able to attach to the top of it, as this is the method that material will be pushed into the nozzle using. Therefore, there must be luer lock connections on the nozzle for the syringe barrels. The dimensions for the luer lock connection are shown in Figure 17 below. Additionally, the design should be capable of expanding to accommodate additional materials, if desired, with 3, 4, or 5 material nozzles easily designed based off the two-material circular nozzle. It also must be

capable of withstanding the pressures used to print, as the material is extruded pneumatically. The carbon nanotube filament is extruded at a pressure of roughly 20-25 psi, so this was used as reference when designing the nozzle. Thus, the designed nozzle based upon these design constraints is shown in Figure 17 below in a fully dimensioned engineering drawing.

Square and circular nozzles were designed for two-material printing, with a conceptual drawing of a square example shown in Figure 18 below. The circular nozzle uses less resin for printing; however, the square nozzle is likely easier to design a nozzle holder for though. The square two-material nozzle was never manufactured or analyzed, with only the circular two-material nozzle analyzed, manufactured, and tested.

As one of the main design requirements for the nozzles is that they be easily manufactured, and ideally easily mass manufactured, they were able to be printed on a resin printer. The chosen printer was a Photon Mono M5s, with the chosen photopolymer resin being Siraya Tech Build Smoky Black Resin. This was chosen due to its high resolution and low shrinkage and warping [25]. Chitubox was used to slice the file for printing. For support generation, the “heavy supports” option was chosen, with all supports generated in the interior volume of the nozzle deleted. Figure 14 below shows an image of the nozzles in the slicing software, with the correct printing orientation and the supports generated. The initial geometry of the two-material nozzle had walls that were too thin near the tip and were difficult to create on the resin printer. The first batch of 15 nozzles with the initial geometry all had the same defect near the tip of the nozzle, with a hole in the wall, with an example shown in Figure 15 below.

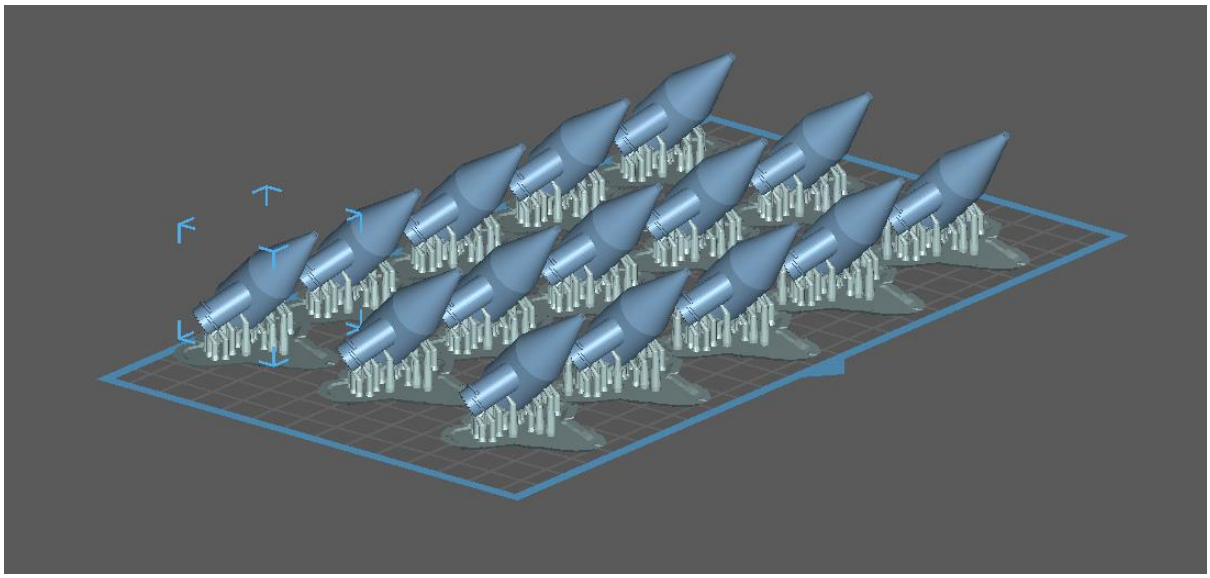

Figure 14: 15 Nozzles in Chitubox Slicing Software with Supports and Printing Orientation

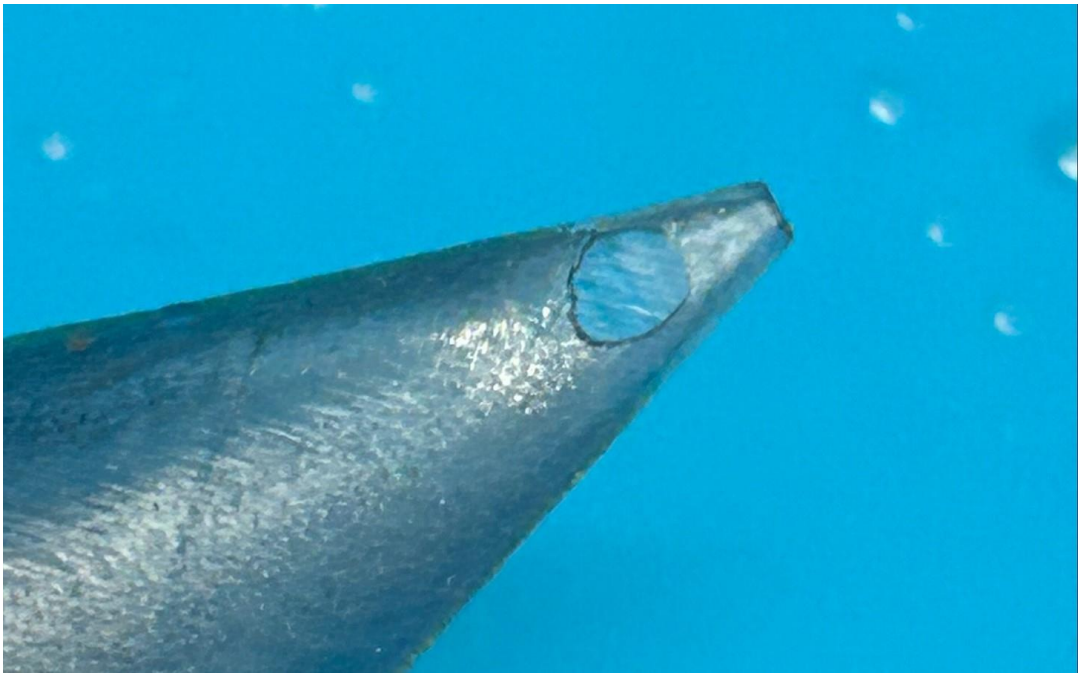

Figure 15: Image of the Defective Nozzle due to Thin Geometry

These holes were fixed by making the outer wall of the nozzle thicker. As the outer wall surface is a loft between the nozzle tip and the point where the nozzle begins tapering, increasing the thickness of the wall at the nozzle tip increases the thickness of the wall overall. The initial wall thickness at the tip was 0.02 inches. After these printing defects, this was doubled to 0.04 inches to make the wall thick enough to successfully be printed. An example of the successfully printed nozzle is shown in Figure 16 below.

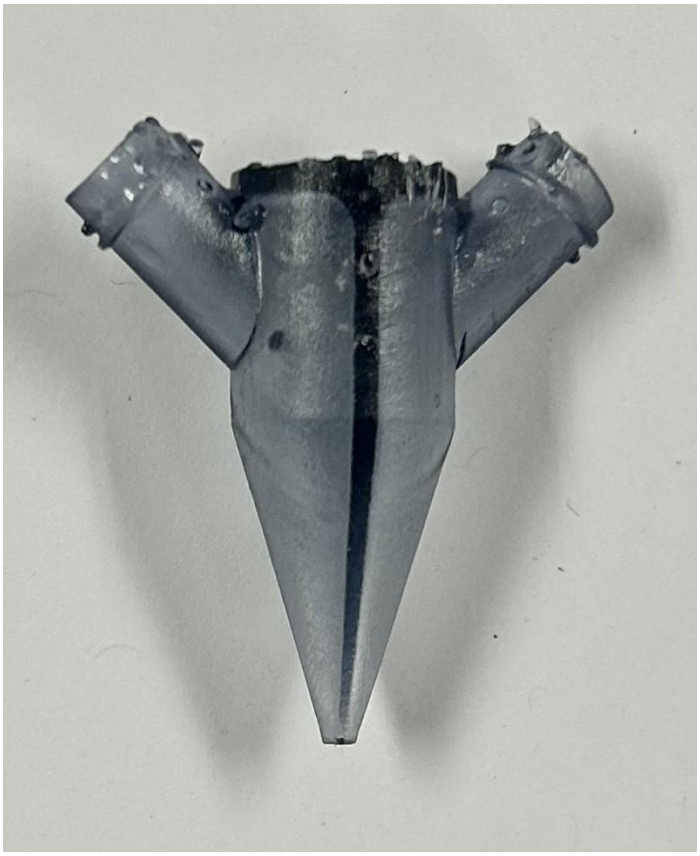

Figure 16: An Example of One of the Successfully Printed Nozzles

Following printing of the nozzle, 5 nozzles were selected to measure the size at the nozzle tip. This was done to check how accurate the tip geometry is, as the nozzle tapers to a point, there is no visual difference in the nozzles if the resin printer failed to

fully create the small geometry at the tip of the nozzle. The outer diameter of the tip of the nozzle, which should be 1.9 millimeters, was measured with a pair of digital stainless hardened nozzles. These results are shown in Table 2 below. These values were all very close to 1.9 millimeters, showing that the resin printer is successfully creating the geometry desired.

Table 2: Tip OD Measurements of Randomly Selected Nozzles

Nozzle	Tip Outer Dimension Measurement (mm)
1	1.89
2	1.91
3	1.94
4	1.93
5	1.89

No nozzle designs were analyzed, manufactured, or tested other than the two-material circular nozzle, and the drawings provided of the other nozzles are intended to only be conceptual sketches.

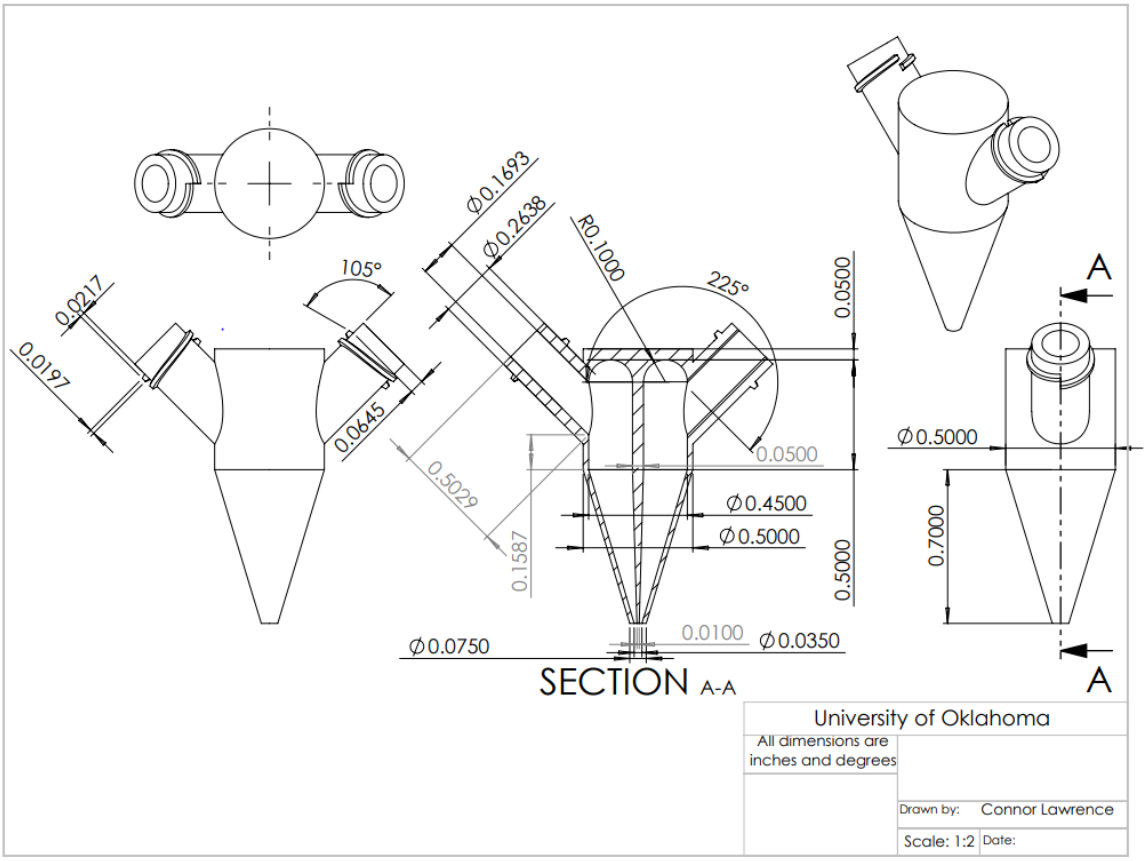

Figure 17: Dimensioned Engineering Drawing of the Circular Two Material Nozzle Design

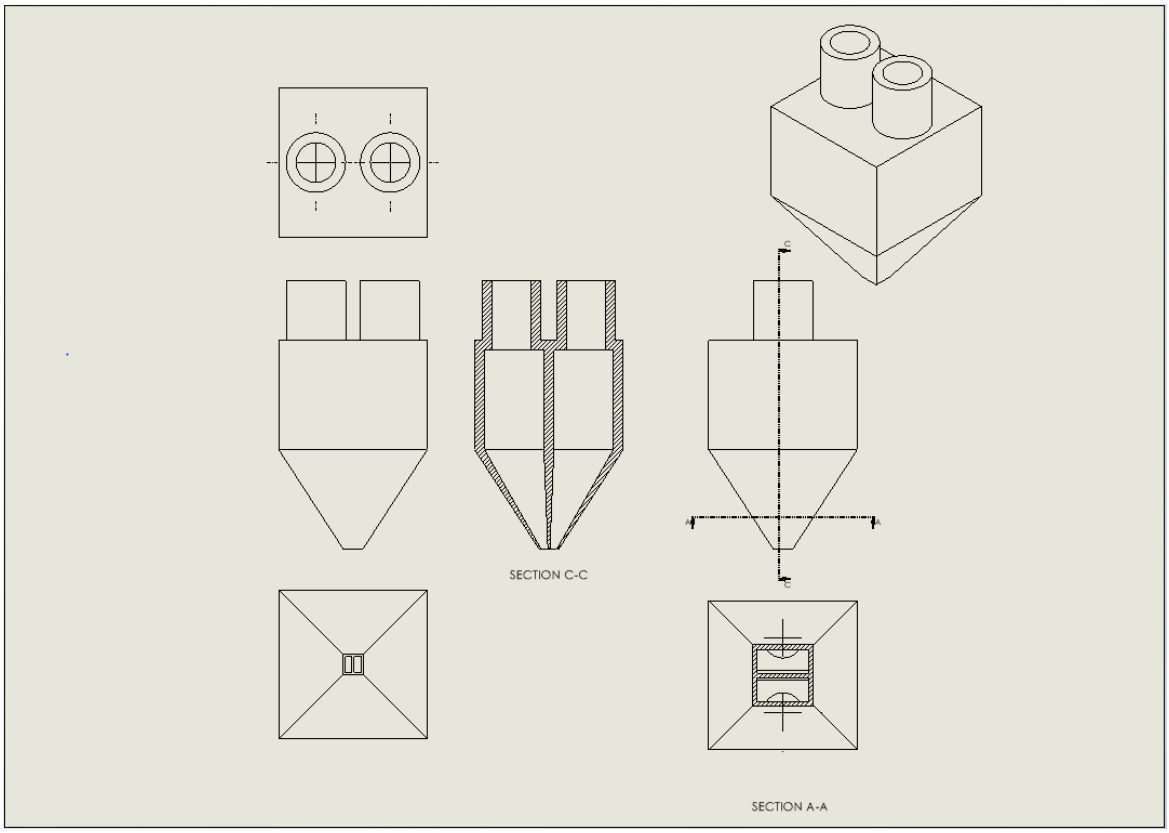

Figure 18: Drawing of the Square Two Material Nozzle Conceptual Design

3.2: 3+ Material Nozzle Design

Since one of the main considerations taken into designing the two-material nozzle was that the design be easily expanded for more materials, other nozzles were designed capable of printing 3, 4, or 5 materials at once. However, these were not tested, due to a lack of pneumatic connections on the modified Ender 3 Printer, and the two-material design was focused on during testing and analysis. Three different geometries were designed, with either a triangle tip, square tip, or a circular tip. The designed nozzles include a three-material concentric nozzle, four-material square nozzle, four-material triangular nozzle, five-material concentric nozzle, and a five-material square nozzle. The design constraints for these are the same design constraints considered

when designing the two-material nozzles. All these nozzle designs are intended to easily be capable of expanding to include the number of desired materials for the print. Conceptual drawings without dimensions of these nozzles have been included in Figures 19-23 below to illustrate the ability of these designs to accommodate the desired number of materials for printing.

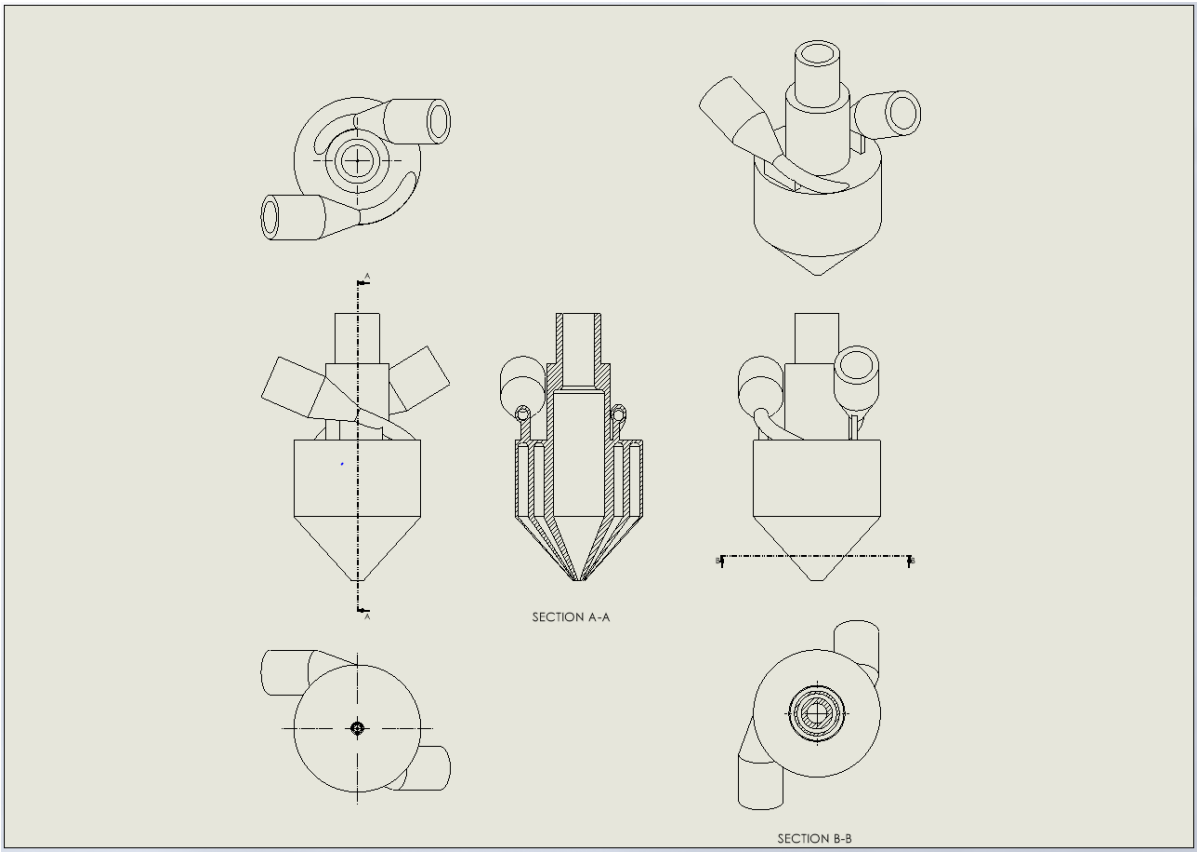

Figure 19: Drawing of the Circular Three Material Nozzle Conceptual Design

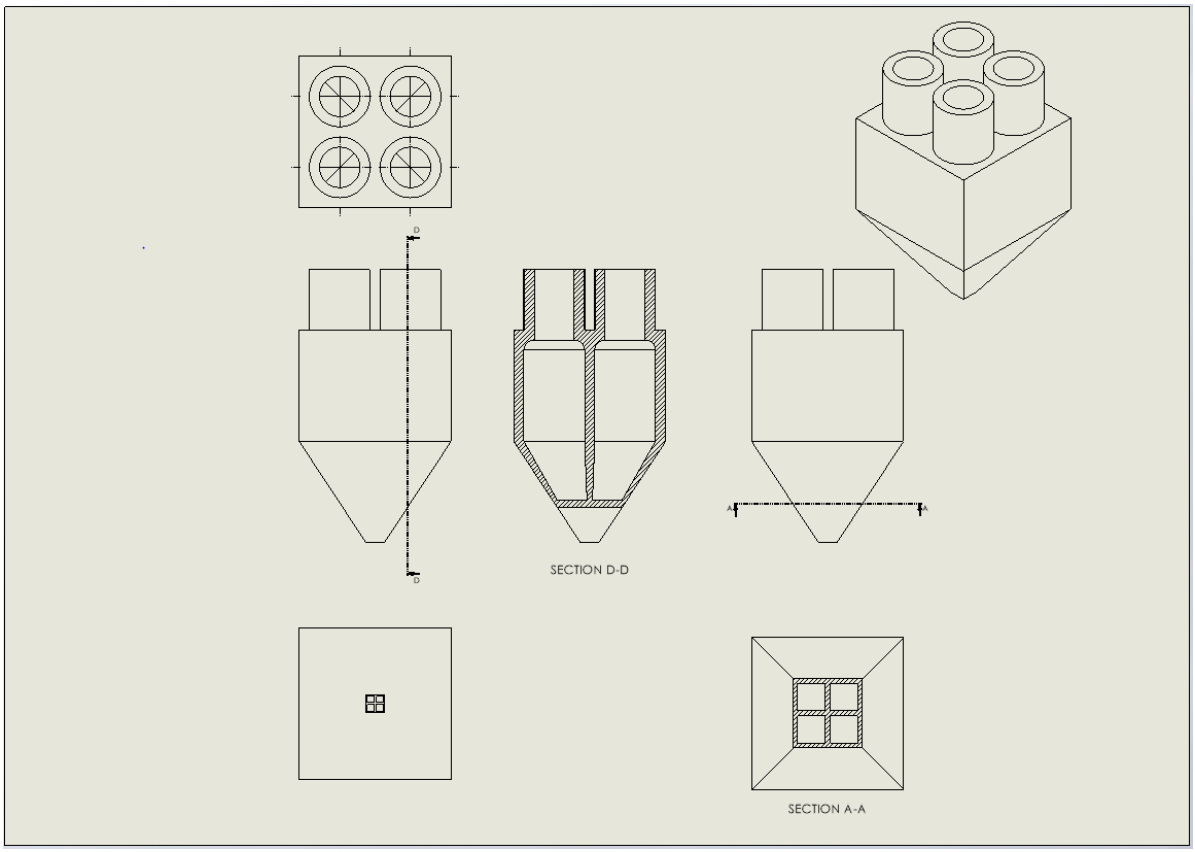

Figure 20: Drawing of the Square Four Material Nozzle Conceptual Design

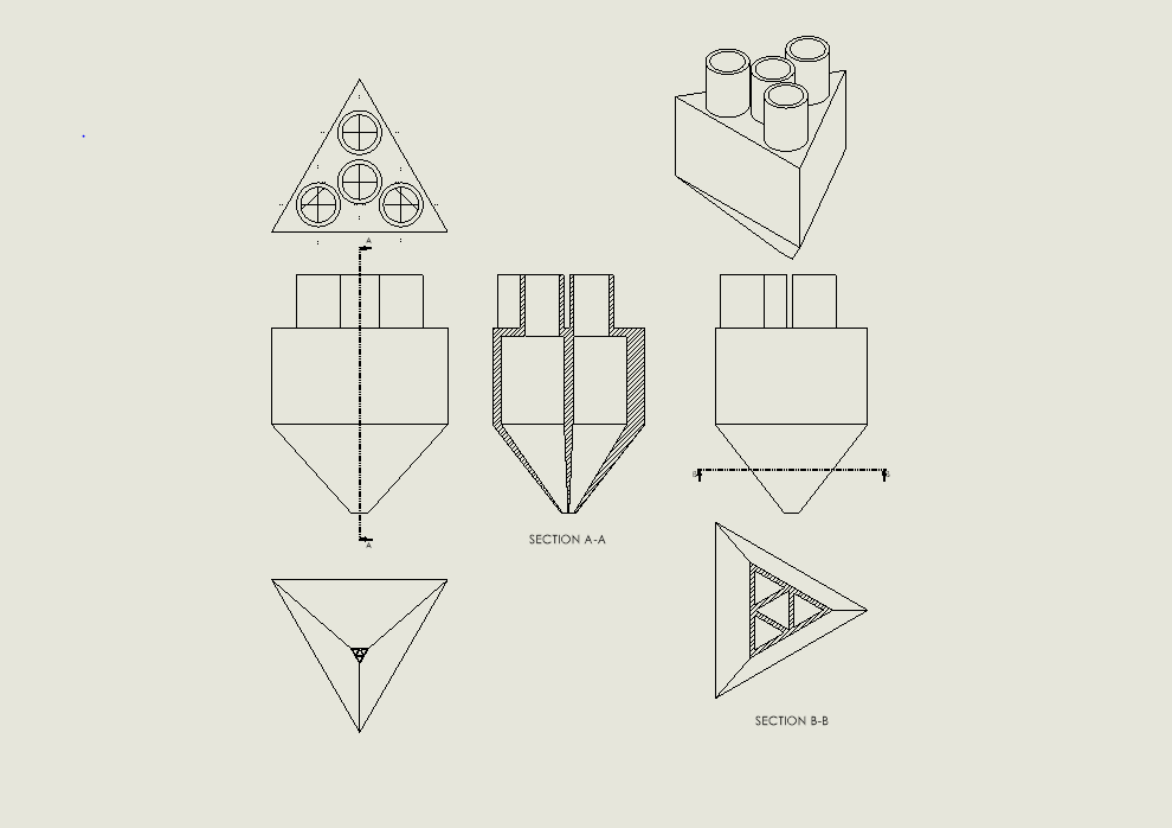

Figure 21: Drawing of the Triangular Four Material Nozzle Conceptual Design

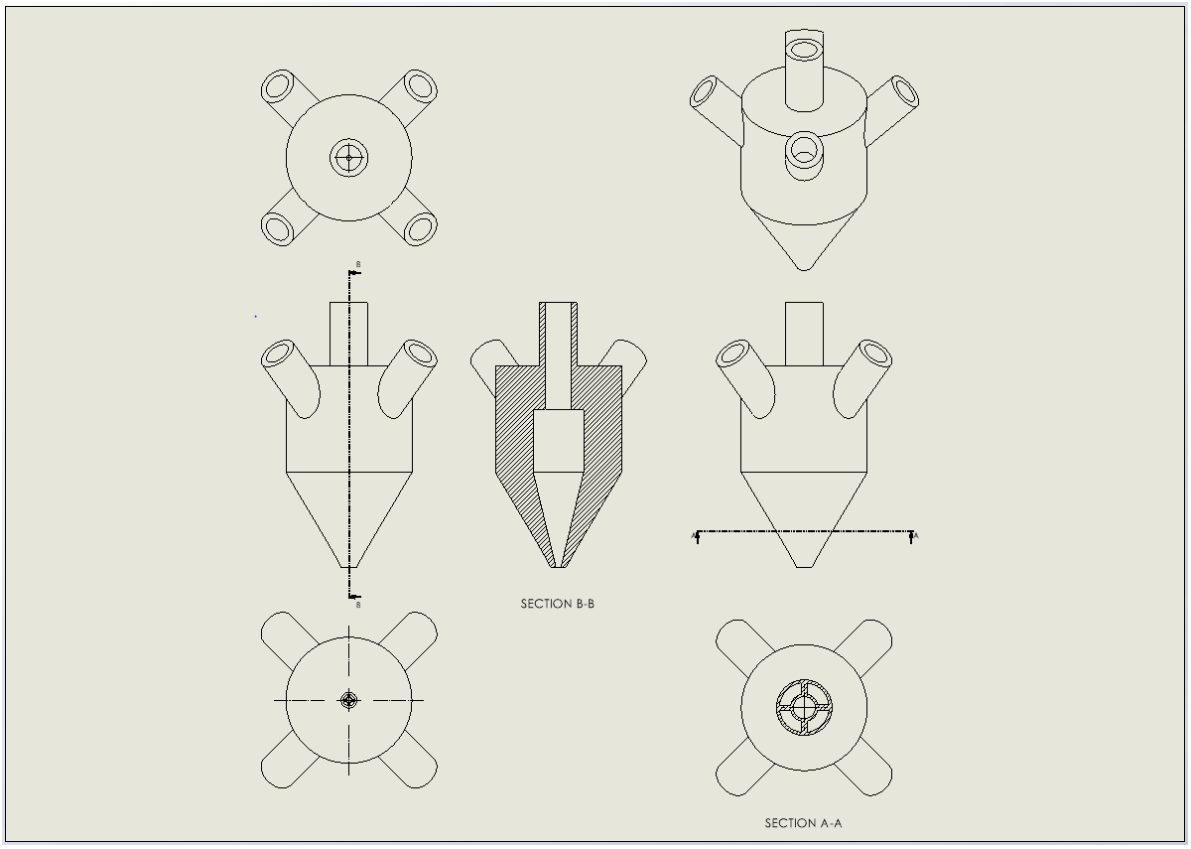

Figure 22: Drawing of the Circular Five Material Nozzle Conceptual Design

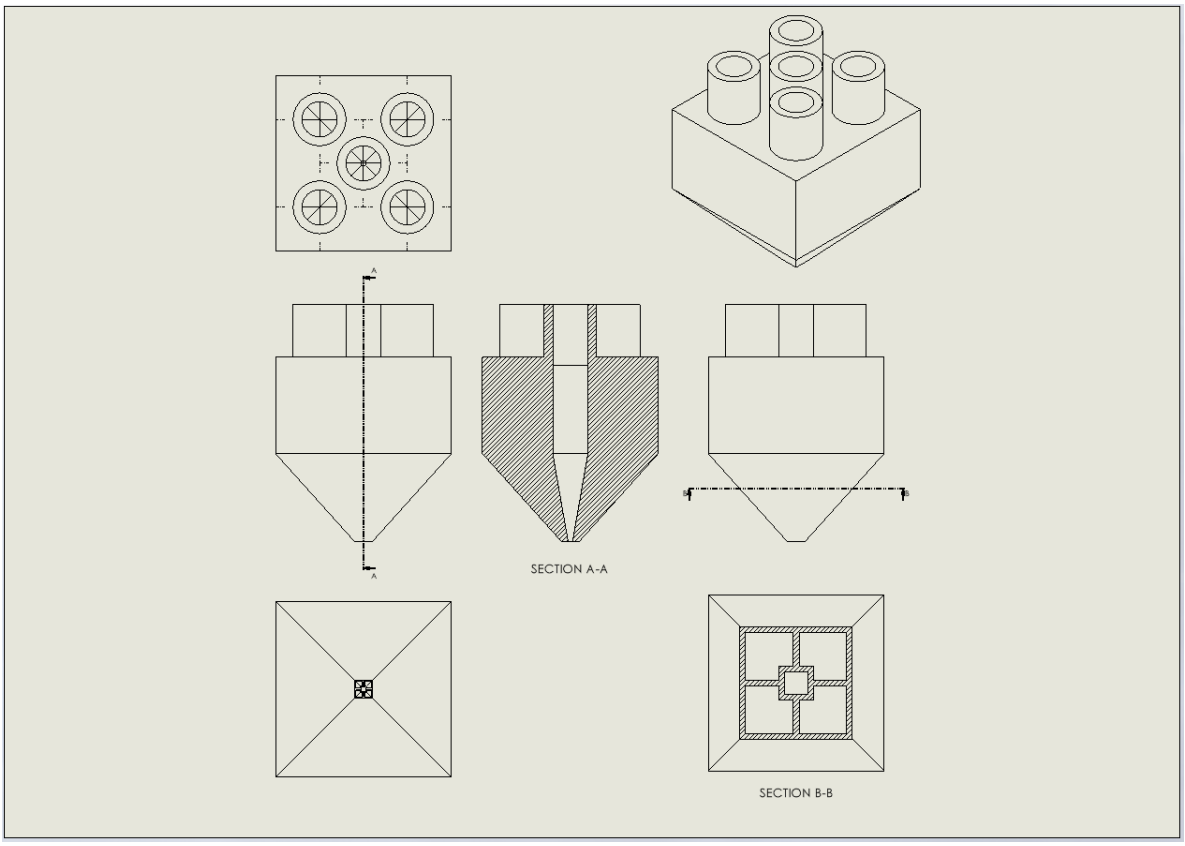

Figure 23: Drawing of the Square Five Material Nozzle Conceptual Design

3.3: Nozzle Holder

Additionally, to hold the nozzle in place while it is printing, a nozzle holder is required for the printer. The nozzle holder is required to be easily manufactured using traditional PLA 3D printing, capable of lowering the nozzle to the print bed to print at Z = 0 and must also be lightweight enough to be able to be controlled using the stepper motor of the 3D printer. The geometry of the printer that needed to be modified to hold the nozzle is shown below, in Figure 24.

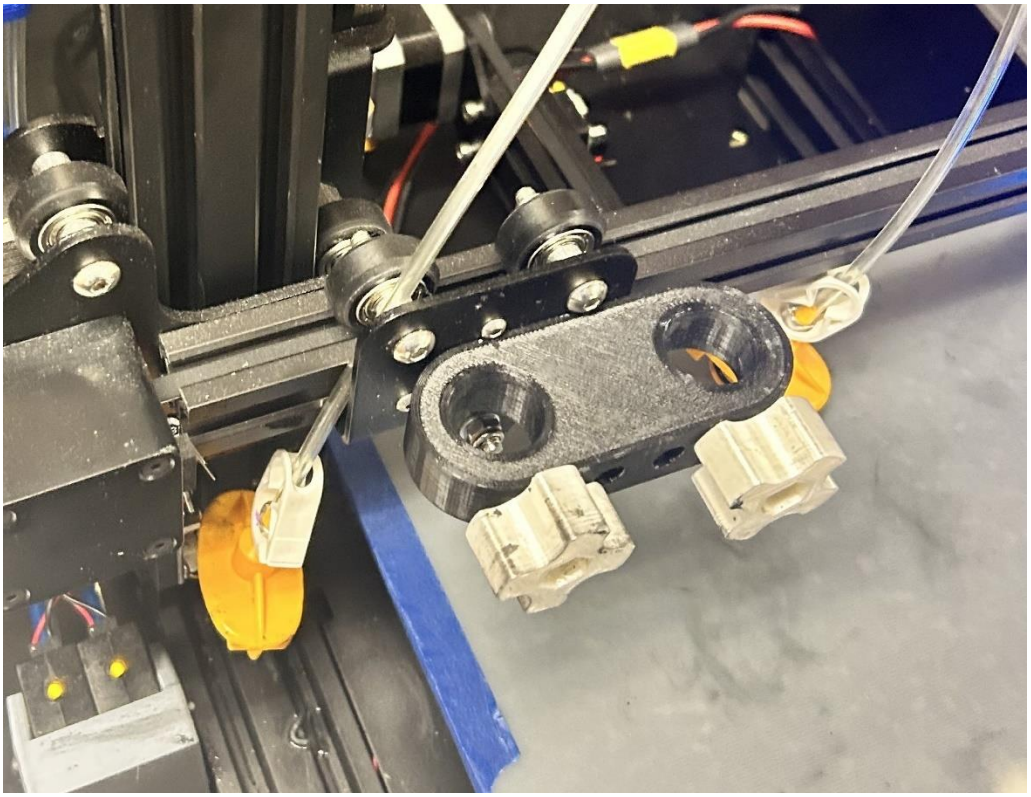

Figure 24: Geometry of the Print Head of the Modified Ender 3 Printer

As seen in Figure 24 above, the printer head and extruder section has been replaced by a black 3D printed holder, bolted to the back plate of the extruder head. On the original black 3D printed holder, there are 2 cylindrical holes, with white knobs with a bolt on the inside to tighten the object placed through the cylindrical holes. While the holes were originally intended to hold syringes, with the white knobs being meant to hold the syringes in place, this can be modified to hold the nozzle holder in place.

The nozzle was designed to be a press fit into the larger vertical hole at the bottom of the holder. A press fit was chosen to hold the nozzle in place as it would not be too difficult to place and remove, while also being capable of holding it steady. The hole of the nozzle holder is an inverse profile of the nozzle itself, tapering down to a point just

like the nozzle, to create the geometry necessary for the press fit. This design was printed using PLA on a FlashForge Creator Max 2, sliced with FlashPrint 5, with 15% infill. The design was a two-part design, with the main section shown in Figure 25 below, and the other section, with the press fit for the nozzle itself, shown below in Figure 26. All dimensions shown in Figures 25 and 26 below are in inches and degrees. They were printed separately to reduce the need for support material, therefore reducing both print time and material. Additionally, the press fit hole has tight tolerances, so it should be printed without needing to remove support material from it. These two parts were attached together using epoxy and resin. Testing with the full mass of printing operations, with full syringe barrels showed that the stepper motors could handle this load.

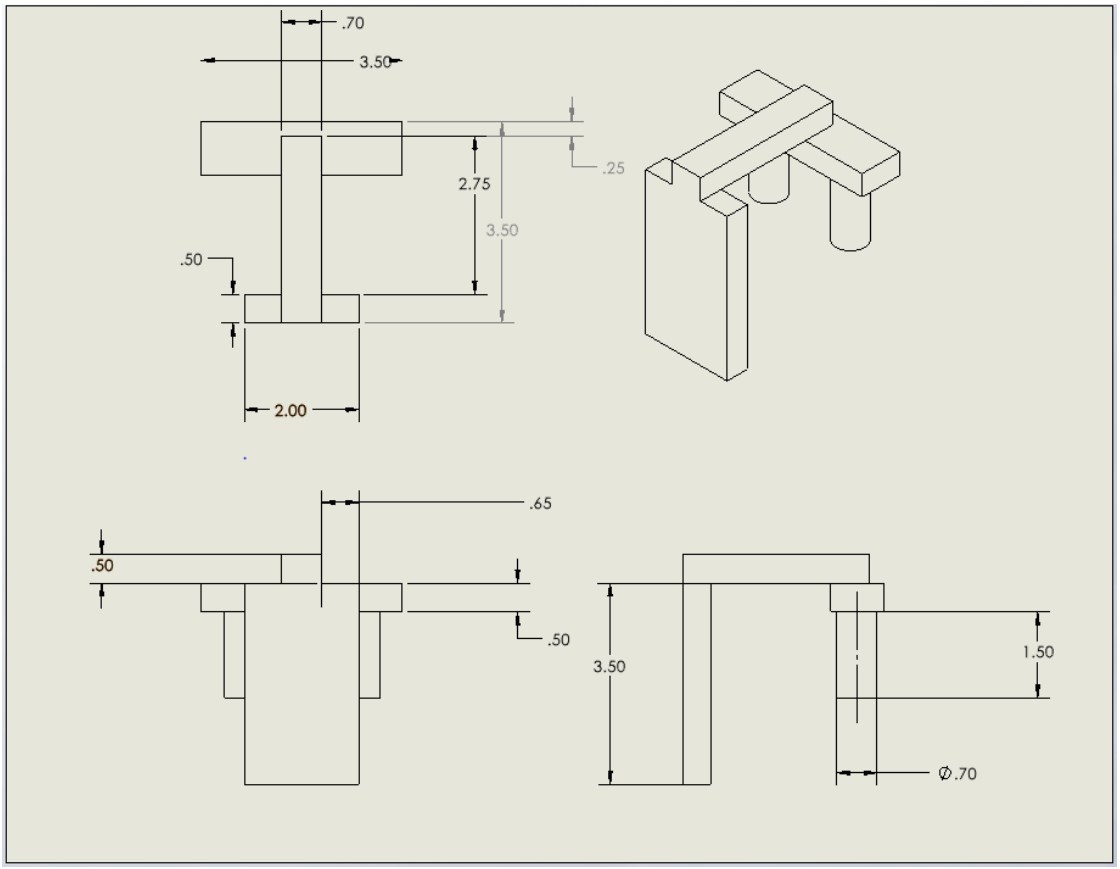

Figure 25: Dimensioned Drawing of the Main Section of the Nozzle Holder

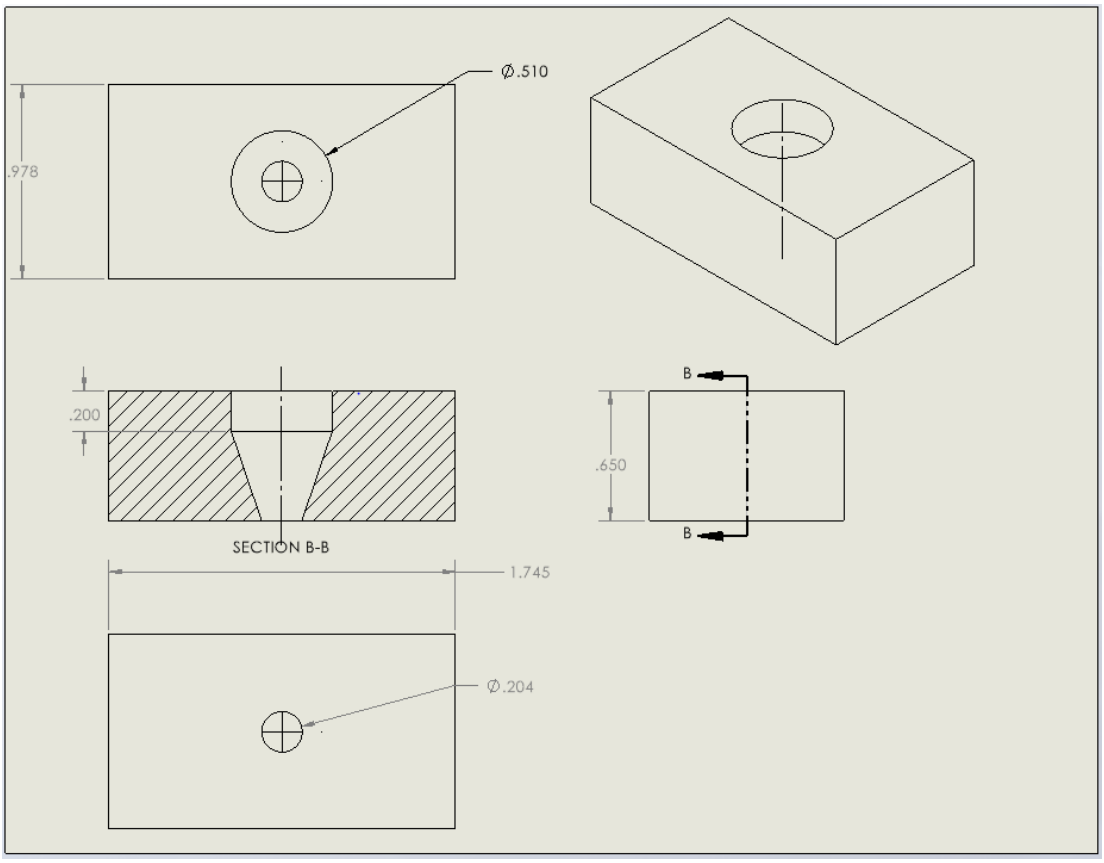

Figure 26: Press Fit Section of the Nozzle Holder

3.4: Structural Analysis of the Nozzle

A structural analysis was also conducted of the nozzle, to show that it would be capable of withstanding the pressures applied during the printing process. Using the results of the rheological study conducted in Chapter 4.4 and the CFD study conducted in Chapter 4.5, the interior wall pressure was simulated to see the maximum stress, maximum displacement, and the minimum safety factor that the nozzle experiences. The interior wall pressure was 3.597e4 Pa, seen when the viscosity was 2500 mPa*s. The structural analysis was conducted using an Ansys static structural analysis, using a student license from the University of Oklahoma.

Material properties of Siraya Tech Build Resin, used to print the nozzle, are summarized in Table 3 below. These properties, along with a value for Poisson's ratio, were uploaded into Ansys to simulate the material for structural analysis. In the Ansys material database, other similar resins have Poisson's ratio values ranging from 0.35-0.4, so a value of 0.35 was selected for this analysis.

Table 3: Material Properties of Siraya Tech Build Resin [26]

Property	Value
Stress at Break (MPa)	33
Young's Modulus (MPa)	850
Water Absorption (24 hr)	2%
Solid Density (g/mL)	1.2

Figure 27 below shows the material properties imported into Ansys for simulation.

1	Property	Value	Unit
2	Material Field Variables	Table	
3	Density	1.2	g cm^-3
4	Isotropic Elasticity		
5	Derive from	Young's ...	
6	Young's Modulus	850	MPa
7	Poisson's Ratio	0.35	
8	Bulk Modulus	9.4444E+08	Pa
9	Shear Modulus	3.1481E+08	Pa

Figure 27: Material Properties for Siraya Tech Build Resin in Ansys

The nozzle geometry was uploaded as a STEP AP203 file. A meshing element size of 0.0005 meters was used, resulting in a total of 71279 nodes and 39216 elements upon meshing. Meshing is shown in Figure 28 below.

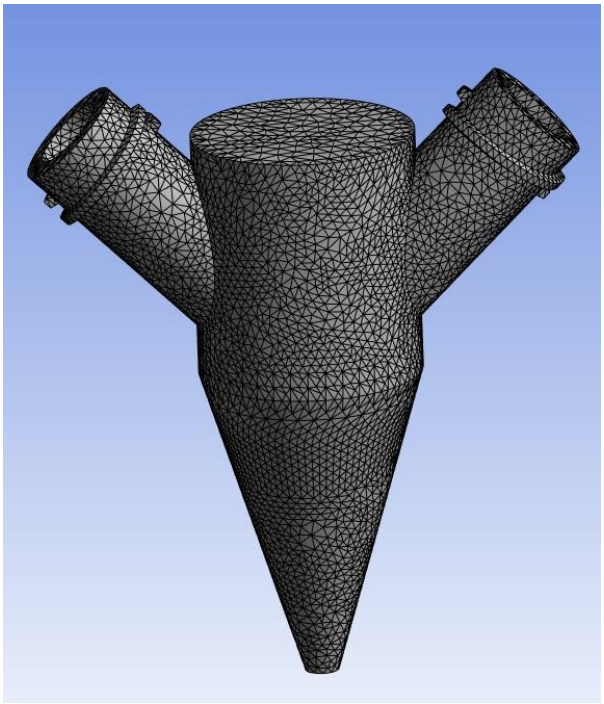

Figure 28: Meshed Nozzle Geometry for Structural Analysis

For analysis, the interior wall pressure found during CFD of 3.597e4 Pa was used. This was applied on all walls of the interior volume of the nozzle. Frictionless supports were placed on the inlet faces and the outlet faces. Figure 29 below shows the surfaces that the wall pressure was applied on, and Figures 30 and 31 show the frictionless supports applied.

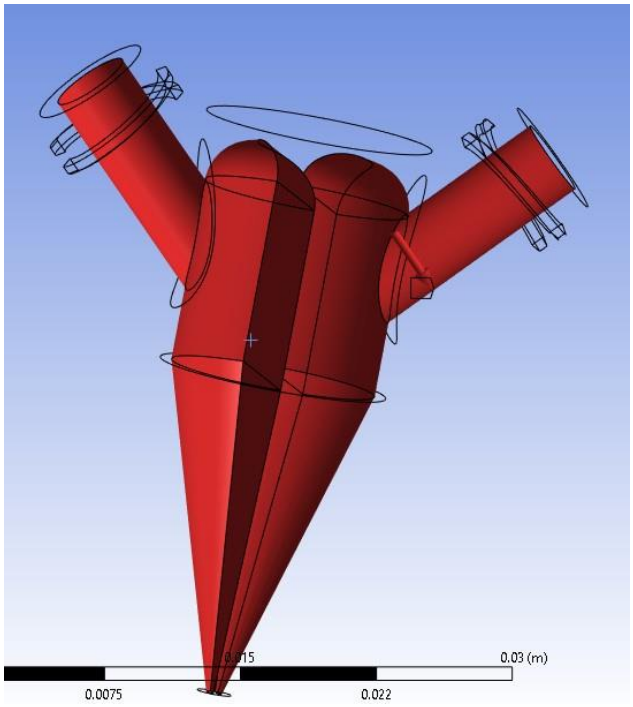

Figure 29: Surfaces that the Wall Pressure was Applied On

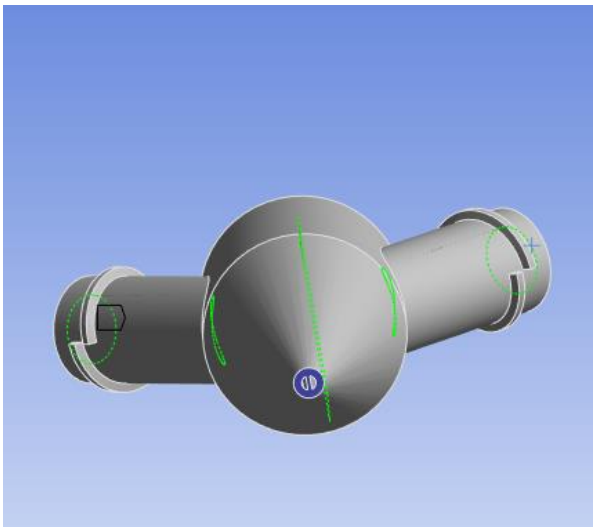

Figure 30: Frictionless Support on Outlet

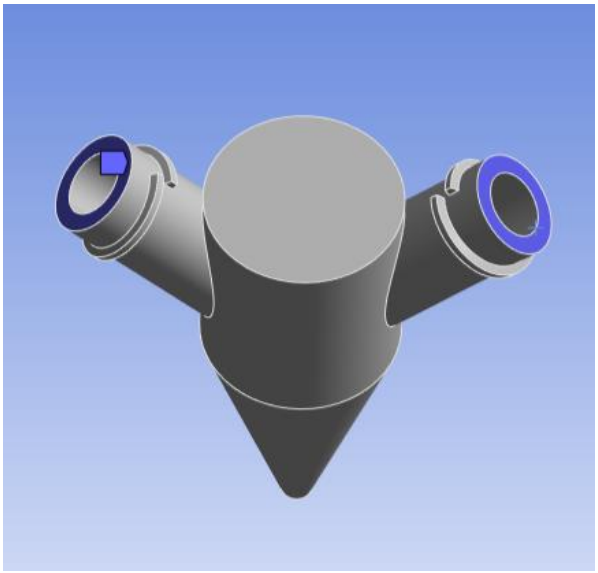

Figure 31: Frictionless Supports on Inlet

The maximum total deformation of the nozzle, as well as the maximum equivalent Von-Mises stress is shown in Figures 32 and 33 below.

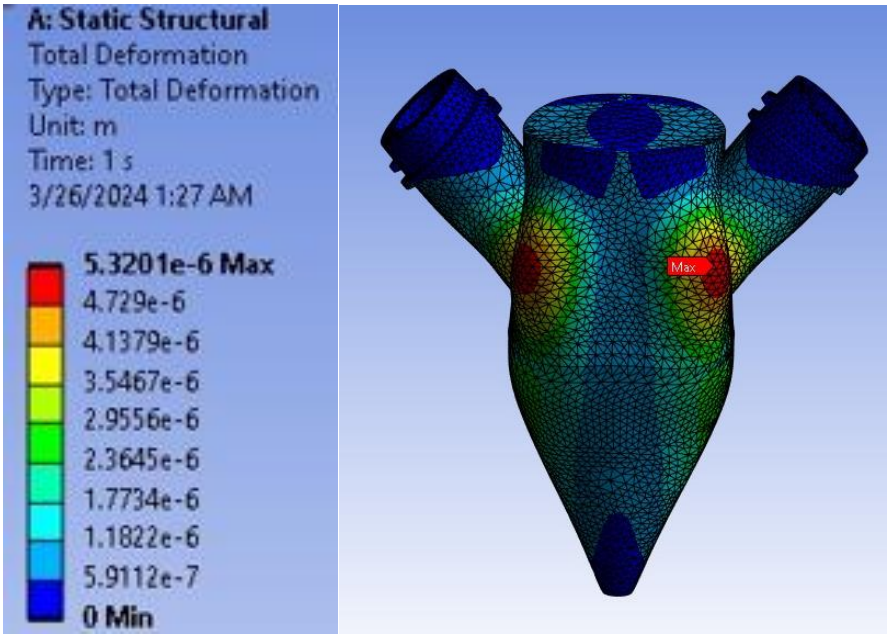

Figure 32: Total Deformation of the Nozzle

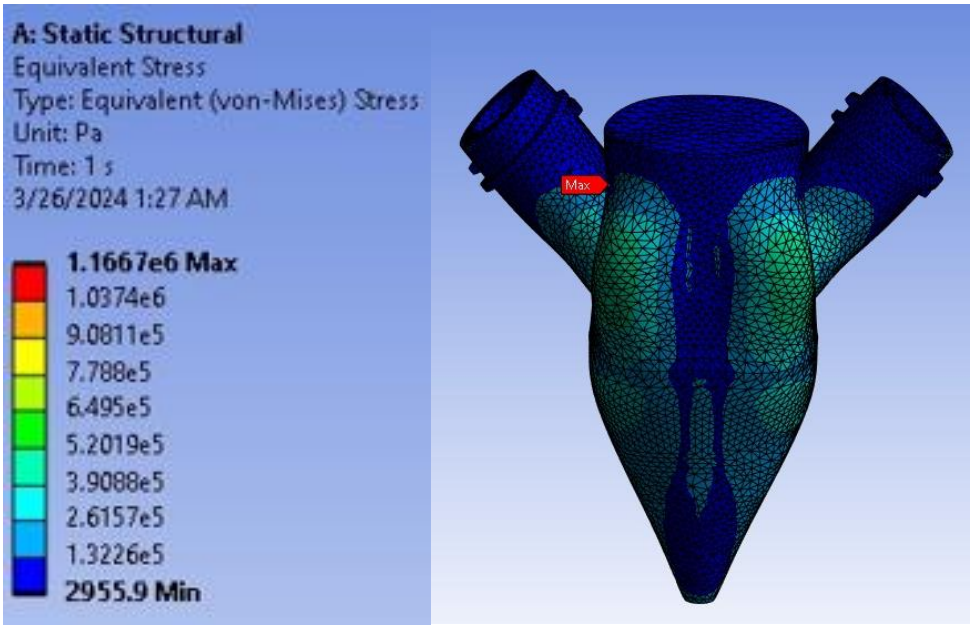

Figure 33: Equivalent Von-Mises Stress of the Nozzle

Given the maximum value of the yield strength of the material from Table 3 above, the safety factor for the nozzle can be calculated. Using equation 1 below, where the σ_{break} is 33 MPa and $\sigma_{von-mises}$ is the maximum stress seen during the structural

analysis, 1.1667 MPa from Figure 33 above, the minimum safety factor of the nozzle can be calculated to be 28.28.

$$(1).\ Safety\ Factor = \frac{\sigma_{von-mises}}{\sigma_{break}}$$

As this value is far greater than 1, the nozzle should not break during operation, and is structurally sound. As seen in the resultant displacement and equivalent stress images by the low values, the nozzle is more than capable of withstanding the forces applied during operation. Additionally, it should be noted, that the fluid is a shear thinning fluid, as described in Chapter 4.4. Thus, as more pressure is applied, more shear forces are applied, lowering the viscosity of the fluid, allowing it to flow easier.

No thermal analysis was conducted, as all print attempts occurred at room temperature, with all materials also being stored at room temperature.

Chapter 4: Printing Results

4.1: Printing Process Overview

The printing process for printing with the designed two material nozzle is like the previous direct ink writing work mentioned in Chapter 2.1. The printer utilized is the same, with the only modifications to the printer itself being the nozzle holder added and described in Chapter 3.3.

The silicon rubber material printed consists of a mixture of 3 chemicals, purchased from Smooth-On, and all used in the printing process described in Chapter 2.1: Eco-Flex 00-30 Part A, Eco-Flex 00-30 Part B, and THI-VEX. This printing process also uses many of the same components and equipment as described in Chapter 2.1, with the only new material being food coloring added to the mixture. Since the nozzle has two connections for syringe barrels to be attached to, two different mixtures must be prepared to utilize the nozzle. Initial tests of the nozzle utilized the same chemical composition of the material for both sides of the nozzle, with the only difference being the color of food coloring added to the mixture. First a black Gejoy Luer Lock Needle Tip Cap was placed over the tip of an IntelliSpense 10cc Clear Pneumatic Syringe Barrel to prevent leakage while mixing the filament. Next, this was placed onto a B303 balance created by Mettler Toledo, capable of measurement to the thousandth of a gram, and 5 grams of Eco-Flex 00-30 Part A was deposited into the syringe barrel using a disposable syringe. This process was repeated with 5 grams of Eco-Flex 00-30 Part B and another disposable syringe. Following this, the THI-VEX was added in the same manner, with the percentage weight of THI-VEX being calculated as shown with example calculations in Table 4 below.

Table 4: Sample Percentages of Percent THI-VEX in the Silicon Rubber Mixture

Grams of Eco-Flex 00-30 Part A	Grams of Eco-Flex 00-30 Part B	Grams of THI-VEX	Percent THI-VEX
5	5	0.15	1.5%
5	5	0.5	5%
5	5	1	10%
5	5	1.5	15%

In each barrel of silicon rubber mixed, food coloring was added. The chosen food coloring was Gourmet Food Coloring Liquid, manufactured by Lianyungang Xinai Food Technology. In the first syringe barrel, 3-5 drops of "grass green" food coloring was added, with 3-5 drops of "grape purple" added to the second syringe barrel. To mix the silicon rubber mixture into a homogenous mixture, first, a Luer Lock Female-to-Female Polypropylene Syringe Adapter, manufactured by Dispense All, was placed on the tip of the syringe barrel after removing the Gejoy needle cap. Next, a 10cc white wiper piston from IntelliSpense was placed to cover the top of the syringe barrel. Then, a disposable 10cc syringe was connected to the other end of the luer lock syringe adapter, with a syringe plunger used to push the liquid between the two syringes. This resulted in the silicon rubber being mixed, closer towards a homogenous mixture. Then, following this, the syringe barrel with the mixture was placed into an AR-100 centrifuge, by Thinky Corporation, using a custom designed syringe holder, displayed in Figure 34 below with another Gejoy needle cap covering the tip of the syringe barrel. In the centrifuge, each syringe barrel was mixed for 5 minutes, followed by a 2.5-minute deaeration condition

to reduce the amount of air and other gases in the filament. The counterweight inside of the centrifuge was set to approximately 45 grams to account for the syringe barrel, filament, and the syringe holder. While the first syringe barrel was in the centrifuge, the second syringe barrel of silicon rubber was mixed using the same process outlined above, except for with purple food coloring instead of green. After being removed from the centrifuge, a bit of material was extruded from the syringe barrel before being attached to the nozzle, to ensure that the material extruded was mixed homogenously. The syringe barrels were first screwed onto the nozzle, with the pneumatic connections then attached on the top of the syringe barrel. The green filament syringe barrel was always placed on the left side (or the negative X direction) of the two-material nozzle. Once the syringe barrels were attached to the nozzle and the pneumatic connections, the nozzle was placed into the press-fit nozzle holder. Figure 35 below shows an image of the printing set-up, ready to begin a print. For all print attempts with the two-material nozzle, the print bed was half of a sheet of printer paper placed onto the existing Ender 3 print bed, as it is cheap, easily disposable, and afforded the ability to easily take images.

Figure 34: Syringe Holder for Centrifuge Use

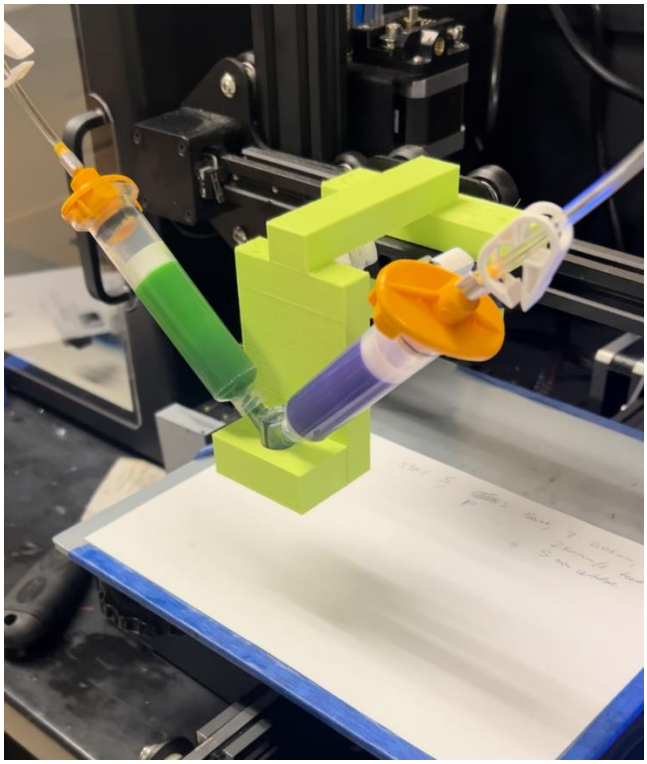

Figure 35: Image of Two Syringe Barrels Attached to the Nozzle and Pneumatic Connections

A resin bath for the print, as utilized in Chapter 2.1, was not used for prints with the two-material nozzle. As no carbon nanotubes were added to the print filament, the material printed as filament for the two-material nozzle is essentially the same material that was used to create the resin bath in Chapter 2.1.

The process of creating G-code for the prints is the same as described in Chapter 2.1, with Prusa Slicer used for geometry and then commands modified by hand to control both the left and right pneumatic valves for the modified Ender 3.

A printing speed of 150 millimeters per second was selected, as this was one of the better printing conditions given in Chapter 4.6. Additionally, 5 psi of pressure was

used, as this is the minimum pressure required to extrude material from the nozzle and worked well with a printing speed of 150 millimeters per second in Chapter 4.6. Printing speed is very difficult to modify mid-print, as the speed of the Ender 3 needs to be increased, however, adjustments to printing pressure are very easy to make mid-print. Therefore, printing speed was kept constant throughout all print attempts, with printing pressure slightly varied.

The nozzles were attempted to be reused after print attempts. Initial reusability attempts focused on using an air hose to blow most of the silicon rubber out of the nozzle, and then an overnight soak in isopropyl alcohol to loosen the remaining silicon rubber and remove residue left behind, followed by using the air hose again to blow the remaining silicon rubber out. To replace the air hose, a G-code was created to simply just blow air through the nozzles for approximately 1 minute to push the remaining material through the nozzle. This was able to successfully remove most of the material from the interior of the nozzle, however, it was not capable of removing all of it. Additionally, a chemical was sought out that would dissolve the silicon rubber that had cured inside of the nozzle following print attempts, however, it would also need to not dissolve the resin that was used for the resin print, as the nozzles were made from resin. Eventually, it was decided to just scrap the nozzles after one use each to save time trying to reuse them, as the nozzle was designed for mass production anyways. If the nozzles were made from a different material, that would enable a chemical to dissolve the silicon rubber but not the material that the nozzle itself is made from, then it would be possible to reuse them. The Photon Mono M5s takes the same amount of time to produce each layer of geometry independent of how much material is cured, as each layer requires an

exposure time to light. Thus, adding additional nozzles to the resin print file does not increase the time of print, only the material required for the print, making mass production of the nozzles on the resin printer easy. Additionally, the technical bulletin for Siraya Tech Build Resin states that the 24 hour water absorption of the material is approximately 2%, and that following printing, the material should not be left in an alcohol solution for more than 5 minutes [26]. As this was not recommended by the manufacturer, an isopropyl soak is likely to damage and ruin the material of the nozzle, meaning a one-time use is likely the best solution with the current material.

4.2: Material Selection

Initial printing attempts focused on geometry that involved printing two squares, approximately 10 millimeters by 10 millimeters, with the distance from the bottom left corner of one square to the bottom left square of the other being 40 millimeters. These are the same squares previously described in Chapter 2.2 and Chapter 2.4. The left side of the nozzle was supposed to be extruding material during the first square on the left, and the right side was supposed to be extruding material during the second square on the right. The first attempts started with a THI-VEX percentage of 1.5%, a print speed of 150 mm/s, and a printing pressure around 5 psi. This initial THI-VEX percentage was chosen based upon the previous usage with THI-VEX to create the bottom layer of the resin bath and used as a basis point for initial tests. It was quickly discovered that the viscosity of the material was not high enough to maintain its consistency upon being deposited out of the nozzle, as seen in Figure 36 below, with the material pooling and translating in both the X and Y directions upon extrusion. Additionally, even with the pneumatic valves closed, material was leaking out of the tip of the nozzle, showing that

the viscosity was not high enough. The filament was sprayed sideways out of the tip of the nozzle, and a pool of filament can be seen below the nozzle that is far thicker in diameter than the nozzle. This shows that the material was not viscous enough for printing, and more THI-VEX needed to be added.

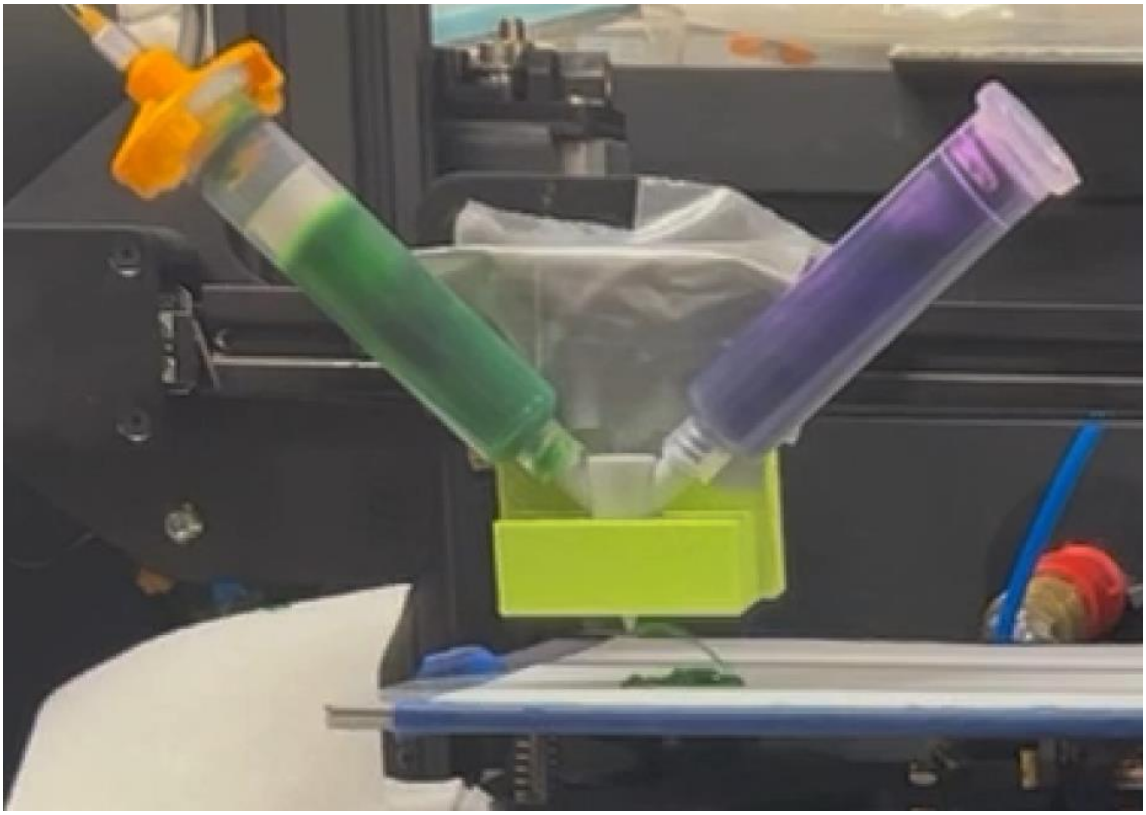

Figure 36: First Print Attempt with 1.5% THI-VEX

Increasing the amount of THI-VEX increases the viscosity, or the thickness, of the printing filament. Due to this, further attempts at printing focused on increasing amounts of THI-VEX, moving from 1.5%, to 3%, 5%, 7.5%, 10% and finally 15%, to find a percentage that resulted in a high enough viscosity to successfully maintain geometry while printing. Print attempts with 3% THI-VEX gave very similar visual results to the print attempts with 1.5% THI-VEX. Material continued to leak out of the nozzle with the

pneumatic valves closed, as well as translate in the X and Y directions upon extrusion. Thus, 5% THI-VEX was attempted and is shown in Figure 37 below.

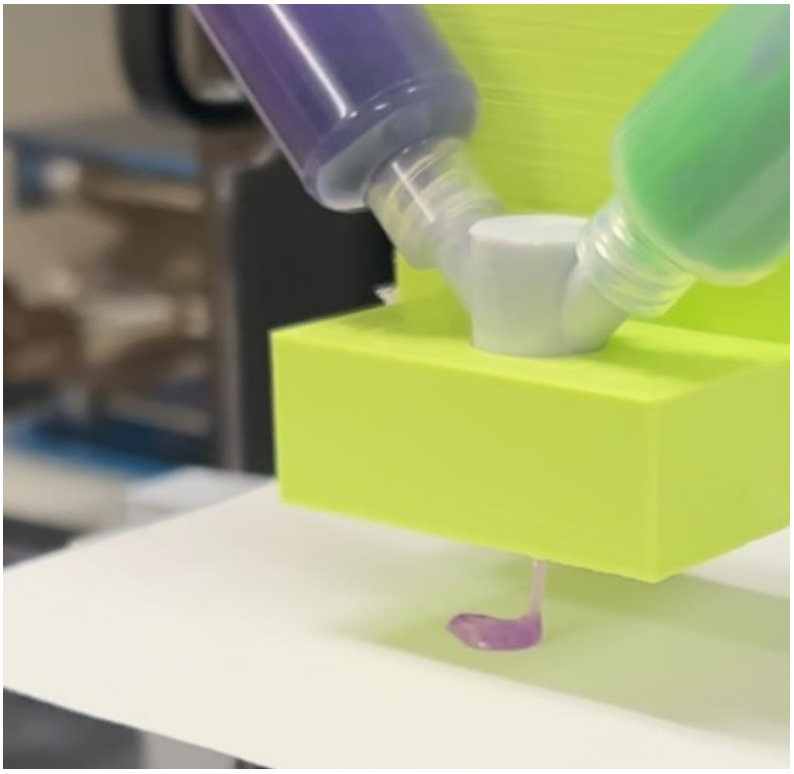

Figure 37: Print Attempt with 5% THI-VEX

As with previous print attempts, 5% THI-VEX resulted in the nozzle leaking material, and the filament translated in the X and Y directions upon extrusion from the nozzle. Next, a print attempt with 7.5% THI-VEX was conducted and shown in Figure 38 below.

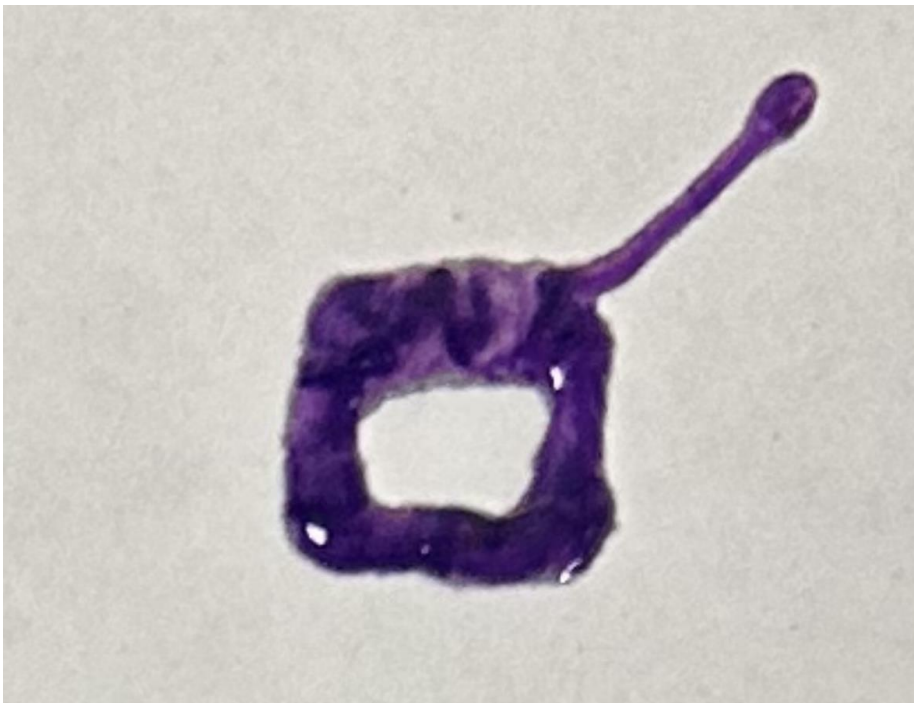

Figure 38: Square Print Attempt with 7.5% THI-VEX

As 7.5% THI-VEX still ran into the same issues described above, a print with 10% THI-VEX was printed and is shown in Figure 39 below. 10% THI-VEX mitigated many of the issues seen previously, however, the nozzle still slightly leaked, leading to 15% THI-VEX as the chosen material upon confirmation that these issues did not persist with the new material composition.

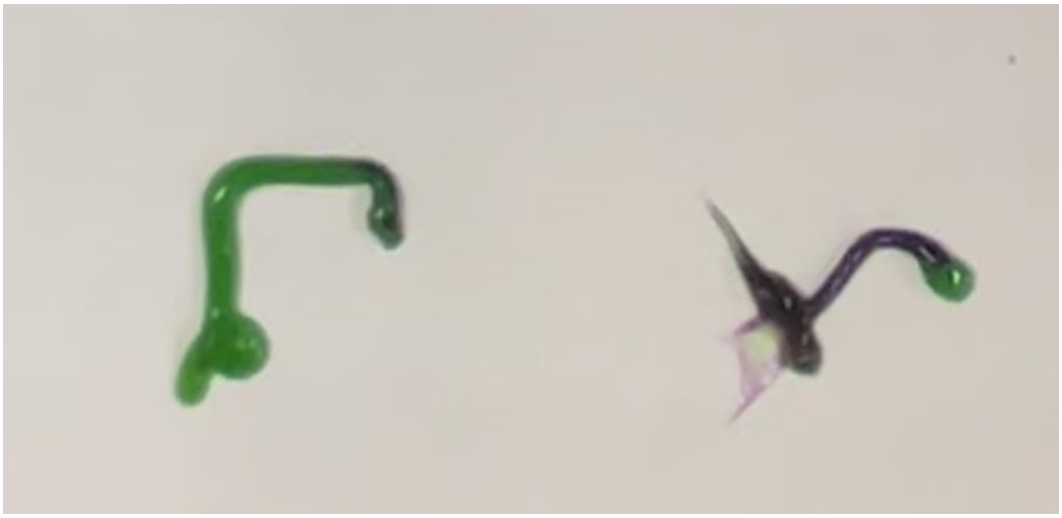

Figure 39: Print Attempt with 10% THI-VEX

4.3: Printing Results

The same star described in Chapter 2.3 was used as complex geometry to evaluate the two-material nozzle. The first print attempts focused on a G-code with only one star, with two printing results shown side-by-side in Figure 40 below. This G-code starts on the bottom left side of the star, moving counterclockwise around the star to print. Initially, too much material is extruded, however, after the pressure is adjusted, the print starts to look ideal near the end of the print. Based upon this, further printing attempts used a G-code with 2 stars, spaced 100 millimeters apart, with the first star intended to be a pressure calibration print attempt. All these prints were conducted with the silicon rubber mixture containing 15% THI-VEX, described in Table 4 in Chapter 4.1.

Figure 40: Initial One Star Print Attempts

Figure 41: First Print Attempt in a Series of Three

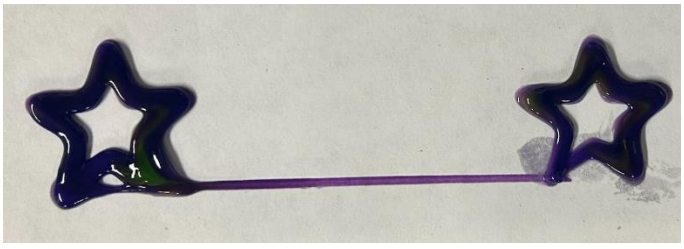

Figure 42: Second Print Attempt in a Series of Three

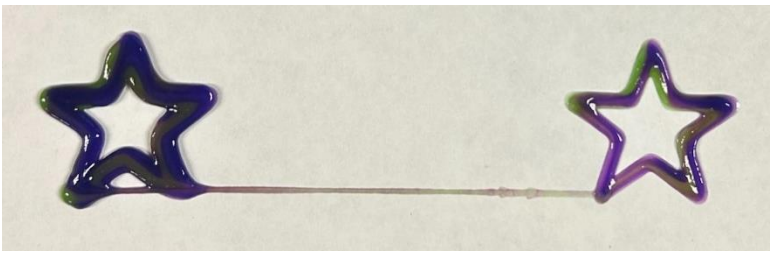

Figure 43: Third Print Attempt in a Series of Three

The three print attempts shown above in Figures 41-43 were printed in series from the same mixture of silicon rubber filament. As seen above, the third print looked better than the first two, with approximately 15 minutes taking place between removing the green silicon rubber mixture from the centrifuge and the third print attempt. Thus, in future print attempts from this point onwards, a 15-minute wait was instituted between the removing the green silicon rubber mixture from the centrifuge and beginning print attempts. This allowed the material to slightly cure before printing, resulting in a slightly higher viscosity, and thus higher quality prints. Two examples of prints created using this new 15-minute wait period are shown below in Figures 44 and 45.

As seen in Figures 44 and 45 below, these print attempts turned out with much higher viscosity of the filament and resemble the desired geometry well. The filament lines are thick and dimensionally accurate to the tip of the nozzle, unlike previous print attempts. Additionally, there is no filament leaking out of the tip of the nozzle when moving from the left star to the right star, as seen in Figures 41-43 above. Once the print was begun with the correct pressure calibrated, the printing pressure did not have to be adjusted throughout the duration of the print.

Figure 44: Two Star Print Attempt with a 15 Minute Wait Period

Figure 45: Another Two Star Print Attempt with a 15 Minute Wait Period

It should also be noted that while never tested on its own, Figures 44 and 45 above show that the nozzle designs can lay down a filament that can be stopped and restarted again. Previously, with a less viscous material with a lower percentage of THI-VEX, and not allowed to cure for 15 minutes before printing, material would leak out of the tip of the nozzle. Figures 44 and 45 showed this to no longer be an issue, therefore increasing the capabilities of the nozzles and the printer.

Additionally, a G-code was created to represent the logo of the University of Oklahoma (OU) to demonstrate a longer print with more complicated geometry. The logo was designed in SolidWorks, then sliced using Prusa Slicer. Following this, the G-code generated by Prusa was adjusted and rewritten by hand to be adapted for the

printer used. The logo is approximately 4 inches in height, and 3 inches wide, with the distance between the two parallel lines throughout the print being approximately 0.11 inches. As the nozzle is 0.035 inches in diameter, without the print looping back in on itself, the geometry should have been able to be created without overlap. The length of this print was 9 minutes and 42 seconds, far longer than the two stars print, which is approximately 90 seconds. Additionally, after the printing pressure was calibrated using another print, the printing pressure was not adjusted throughout the duration of the printing of the OU logo. This proved that the two-material nozzle is capable of greatly increased print durations. Figure 46 below shows the G-code plotted, to visualize what the resultant print should look like, compared to Figure 47, the print results of the OU logo. As seen in Figure 47 below, the printer was able to lay down a continuous filament with approximately the same diameter throughout the duration of the print. Due to the nature of the print, the G-code looped back over itself in a few places, resulting in thicker geometry in those locations, such as where the O and the U meet. The filament was constantly extruded throughout the duration of the print with a consistent, thick line extruded. Both green and purple filament can be seen side-by-side in all parts of the logo, meaning that both materials were successfully extruded without issue throughout the entire duration of the print. This print shows that more complicated geometry with longer duration prints is more than capable of being created using this printing method.

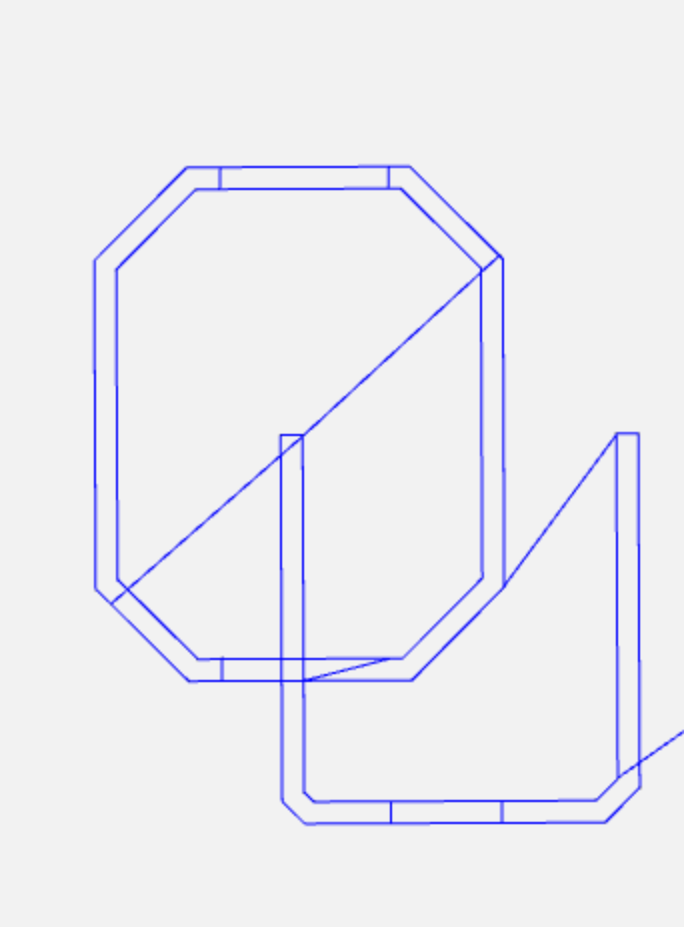

Figure 46: Visualized G-code of the OU Logo

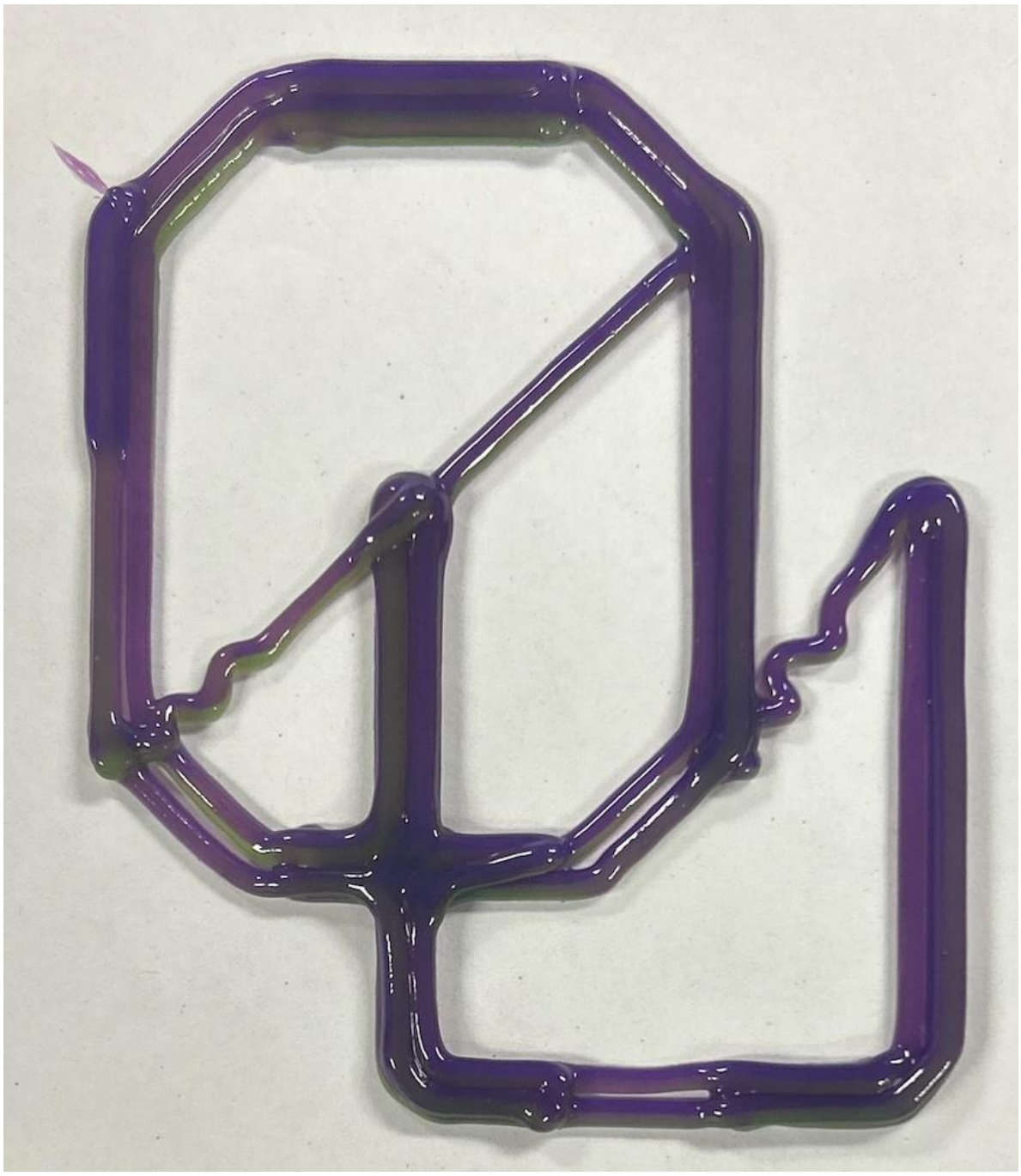

Figure 47: OU Logo Printed Using the Silicon Rubber Mixture and Multi-Material Nozzle

4.4: Rheological Study

A rheological study was also conducted of both the silicon rubber material tested in the multi-material nozzles, as well as the carbon nanotube material used for initial DIW attempts to characterize them. Both materials were mixed in the same method that was used for all print attempts for the rheological study. Rheology is the study of how materials that are neither ideal solids nor ideal liquids deform when forces are applied to them. They display both elastic and viscous reactions to applied stresses, with the goal of rheological experiments to quantify these responses. For solid materials, tensile tests can characterize ideal solids, with elastic moduli calculated from the ratio of stress to strain applied. To characterize viscoelastic properties of complex soft materials, the relation of stress to strain must be applied and measured by a rheometer, and characterized over a wide range of strains, strain rates, and time scales. Rheometers generally measure stress applied to the sample, and the resultant strain deformation of the material [27].

The rheometer used to conduct this study was an Anton Paar MCR 72, courtesy of Dr. Yijie Jiang's lab at the University of Oklahoma. The software used to control the rheometer is the Anton Paar RheoCompass 1.31. This rheometer uses two parallel plates, with a gap height of approximately 0.050 millimeters. First, the rheometer is zeroed. Following this, the upper plate is raised to a height of 60 millimeters to load the sample onto the lower plate. Once the sample is loaded, the upper plate is lowered back into position to perform the tests, at a gap height of approximately 0.050 millimeters. The rheometer has temperature control abilities, but this was not utilized for these tests, with the specimens tested at room temperature. The two tests ran on the materials were

called “Flow curve, logarithmic”, and “Linear viscoelastic range”. “Flow curve, logarithmic”, would measure the viscosity of the fluid as shear is applied, allowing the fluid to be characterized as either shear-thinning, Newtonian, or shear-thickening. The “Linear viscoelastic range” test is an amplitude sweep test that provides the storage and loss modulus of the material vs shear strain.

The first test conducted was the logarithmic flow curve to provide the viscosity – shear rate graph for the sample. The rheometer applies a shear stress, and measures the resultant shear rate, calculating viscosity by dividing the shear stress by the shear rate [28]. 50 measurements were taken, with shear rates up to 2000 sampled. The graphs were created using a logarithmic scale for both the X and Y axes, as the highest rates of change in viscosity usually occur at very low shear rate values [28]. There are 3 types of fluids: shear-thinning, shear-thickening, and Newtonian. Shear thinning inks show a decrease in viscosity when placed under stress, with shear thickening inks increasing in viscosity when placed under shear. A Newtonian fluid exhibits a constant viscosity when placed under stress, with the stress having no impact on the viscosity of the fluid. The most common type chosen for 3D printing is a shear thinning fluid, as it can flow easier when shear forces are applied to it [29]. Since shear forces are present in the printing process, this is more viable than a shear thickening fluid. The shear forces present in 3D printing a shear thickening fluid can cause clogging of the nozzle and the material to clump up, resulting in uneven flow of material. The shear-thinning behavior is desirable during extrusion through the nozzle, as it flows easier, and then rapid recovery behavior of the fluid results in the inks quickly achieving enough strength to rest in place after printing [30]. A shear-thinning fluid is desired over a shear-thickening fluid for 3D

printing, as the printing process provides shear forces to the fluid. If the fluid's viscosity increases when these shear forces are applied, then more shear forces are required to print the fluid, further increasing the viscosity, and so on. As a result of this, either a shear-thinning, or a Newtonian fluid is preferred for 3D printing over a shear thickening fluid. As seen in Figures 48 – 50 below, the tested inks, both the silicon rubber and the carbon nanotube mixture are shear-thinning fluids.

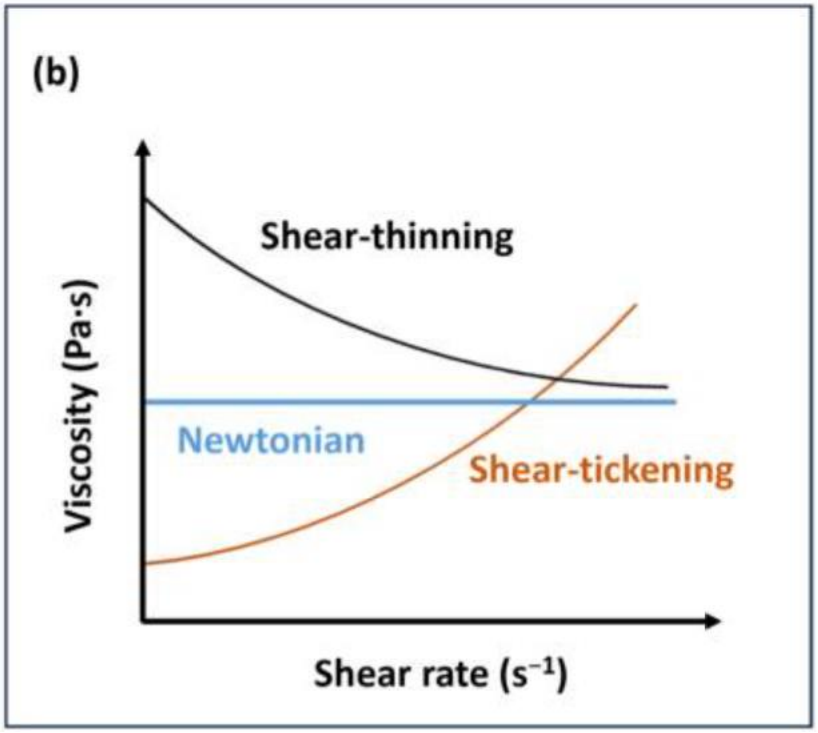

Figure 48: Classification of a Fluid on a Viscosity – Shear Rate Graph [31]

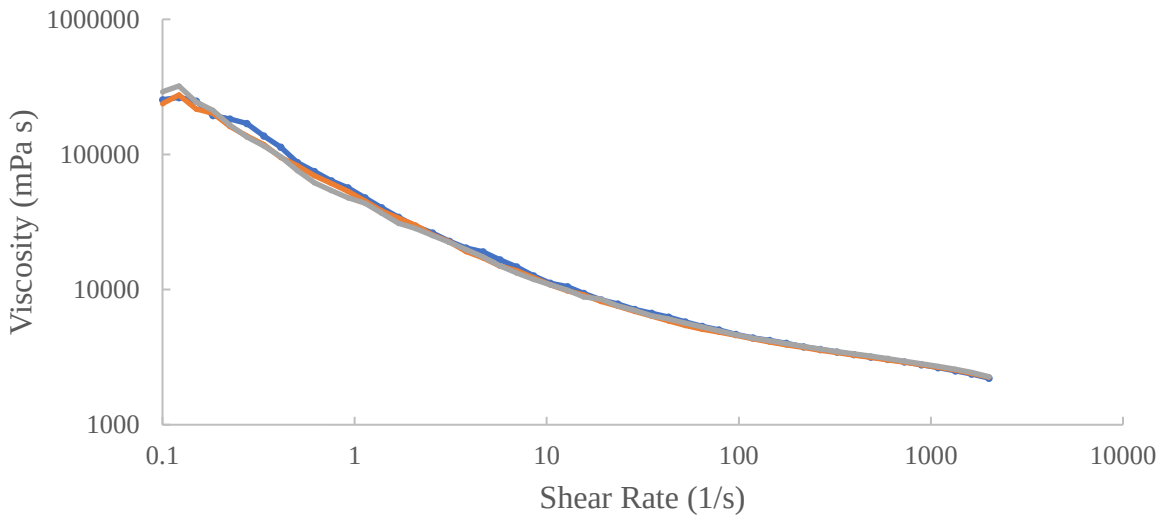

Figure 49: Viscosity – Shear Rate Graph of the Three Samples of Silicon Rubber

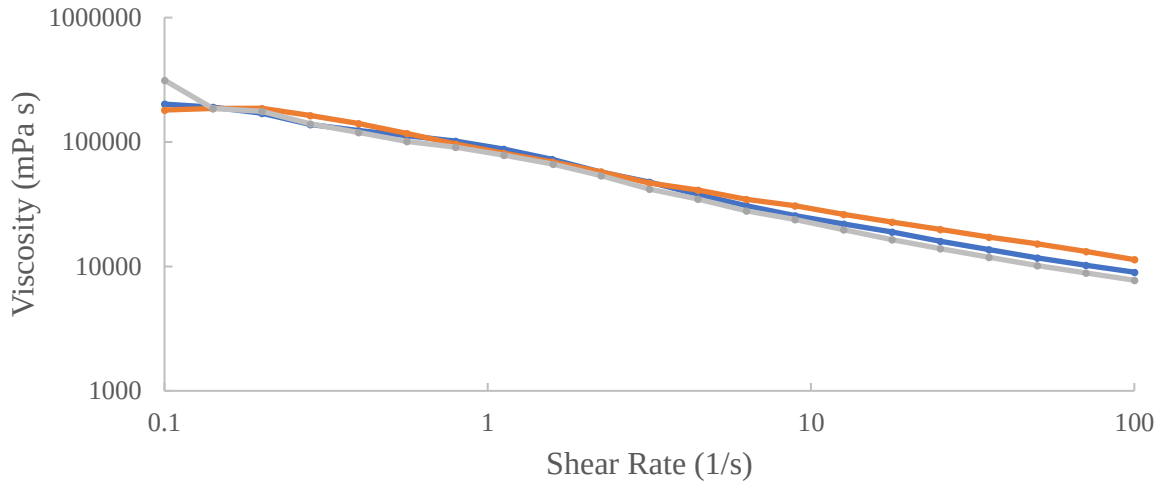

Figure 50: Viscosity – Shear Rate Graph of the Three Samples of the Carbon Nanotube Mixture

As shown in Figures 48 – 50 above, both materials are shear-thinning. The silicon rubber mixture had a viscosity that was lower than the carbon nanotube mixture, throughout the shear rate-viscosity curve. However, it also had a much steeper slope than the carbon nanotube mixture.

An amplitude sweep was also used to evaluate the storage modulus and loss modulus of the material vs shear strain. These graphs are shown in Figures 51 - 56 below for the two tested materials. According to Herrada-Manchon et al, amplitude sweeps are obtained by subjecting the sample to a range of deformations, from 0.1%-1000%, at a fixed frequency, between 0.1 and 1 Hz [32]. Default parameters for the test were used, with none of the parameters changed. The logarithmic nature of the graphs helps visualize the linear viscoelastic region of the material. Herrada-Manchon et al describes this region as the range in which an oscillatory rheology test can be performed without destroying the sample [32]. It is approximately the shear strain values where the storage modulus values stop being approximately constant. It can be seen on the graphs below in Figures 51 - 56 as the point where the storage modulus value starts decreasing downwards. The linear viscoelastic region is also important because it allows the sample to be evaluated amongst the viscoelastic nature of the sample. When the storage modulus is greater than the loss modulus, the sample displays a more solid structure, as it is in the viscoelastic solid region. This displays the gel like behavior of the sample. When the loss modulus is greater than the storage modulus, the sample displays more of a liquid state, as it is within the viscoelastic liquid region of the sample [32]. The polymer has both liquid and solid like features. The storage modulus is representative of the elasticity, whereas the loss modulus represents the energy dissipation of the material

from molecular friction [33]. If the storage modulus was higher than the loss modulus at all shear strains, then the material would behave more like a solid, and if the loss modulus was higher than the storage modulus at all shear strains, then the material would behave more like a fluid. When the loss modulus meets the storage modulus, it is called the crossover point, or the transition from solid to liquid dominant behavior in the material. This is representative of when the material is extruded from the nozzle during 3D printing. According to Than et al, the polymer's storage modulus must not be too high to clog the nozzle and block extrusion, but also not too high of a loss modulus in order to allow the material to retain its shape and not flow freely out of the nozzle [33]. As seen in Figures 51 - 56 below, the two tested samples, the silicon rubber mixture, and the carbon nanotube mixture both meet this criterion for the storage and loss modulus.

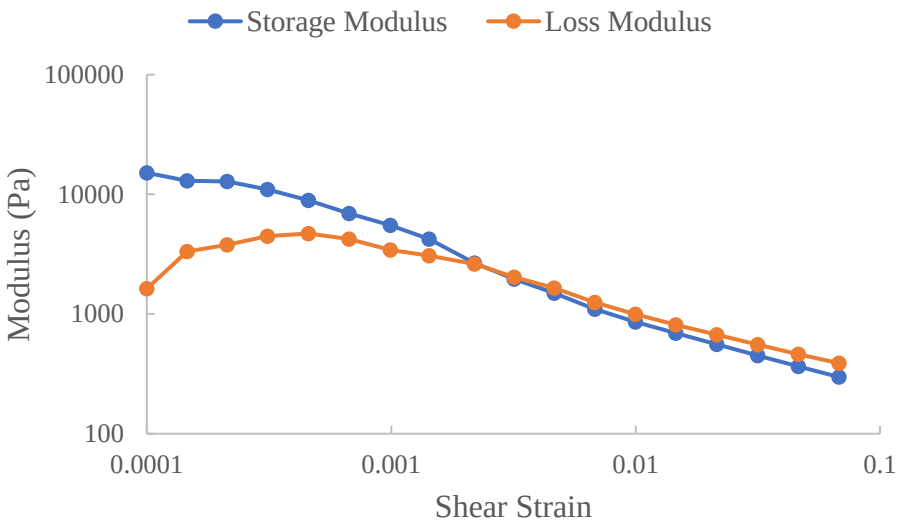

Figure 51: Storage and Loss Modulus vs Shear Strain for Sample 1 of the Silicon Rubber Mixture

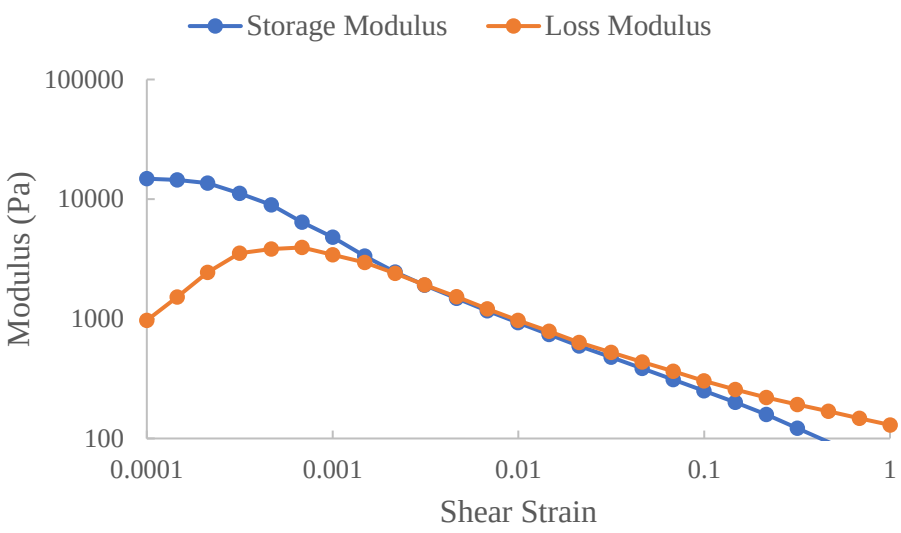

Figure 52: Storage and Loss Modulus vs Shear Strain for Sample 2 of the Silicon Rubber Mixture

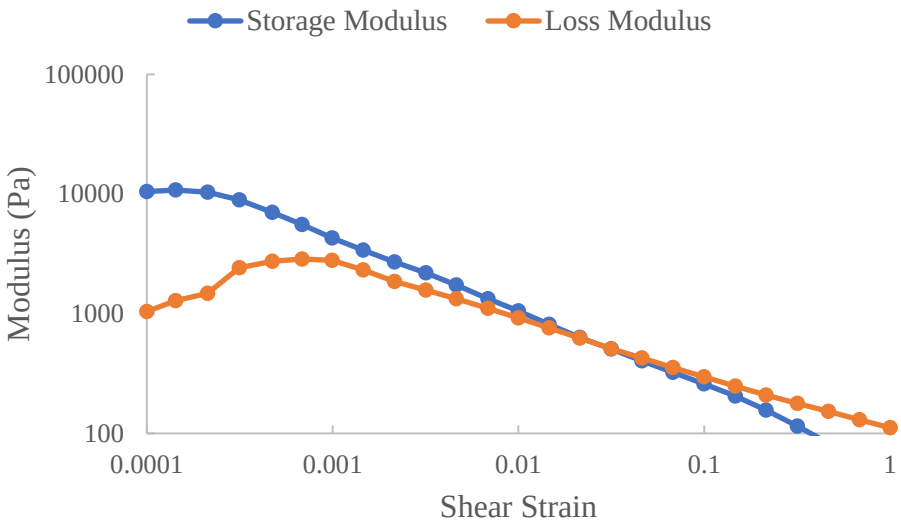

Figure 53: Storage and Loss Modulus vs Shear Strain for Sample 3 of the Silicon Rubber Mixture

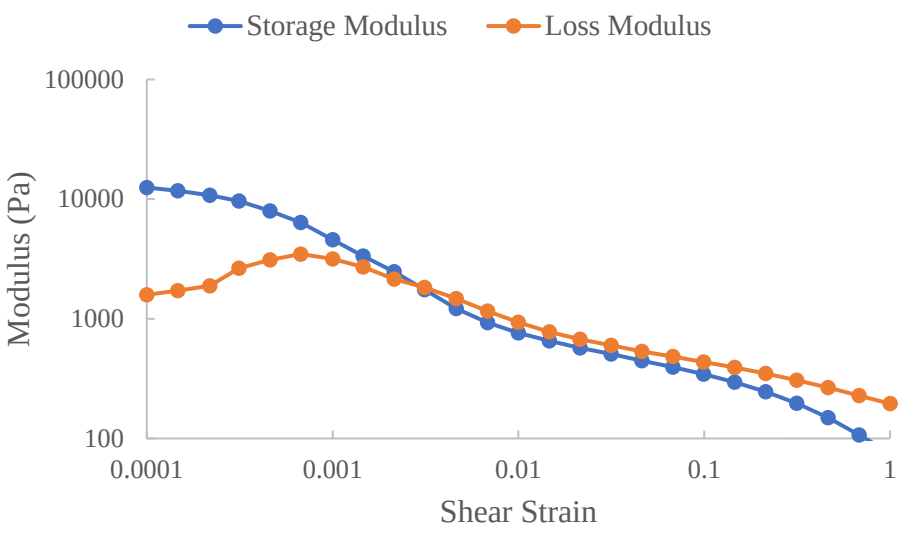

Figure 54: Storage and Loss Modulus vs Shear Strain for Sample 1 of the Carbon Nanotube Mixture

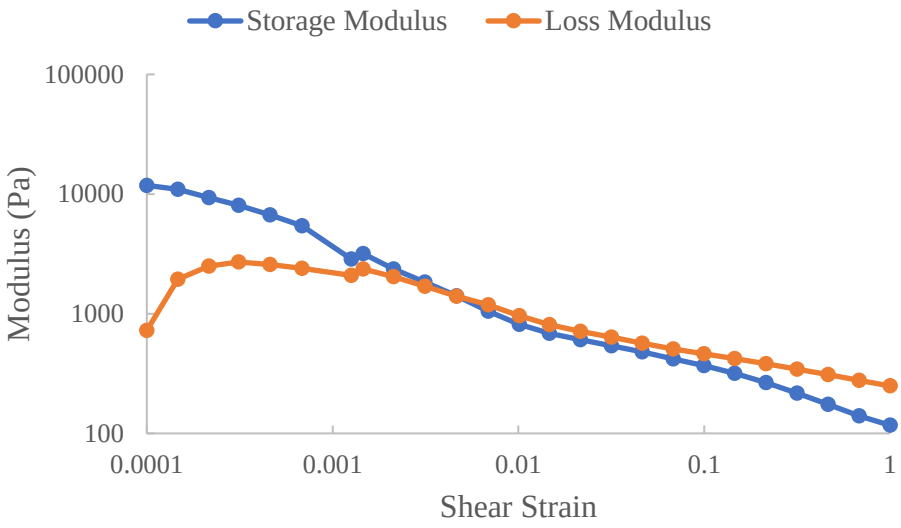

Figure 55: Storage and Loss Modulus vs Shear Strain for Sample 2 of the Carbon Nanotube Mixture

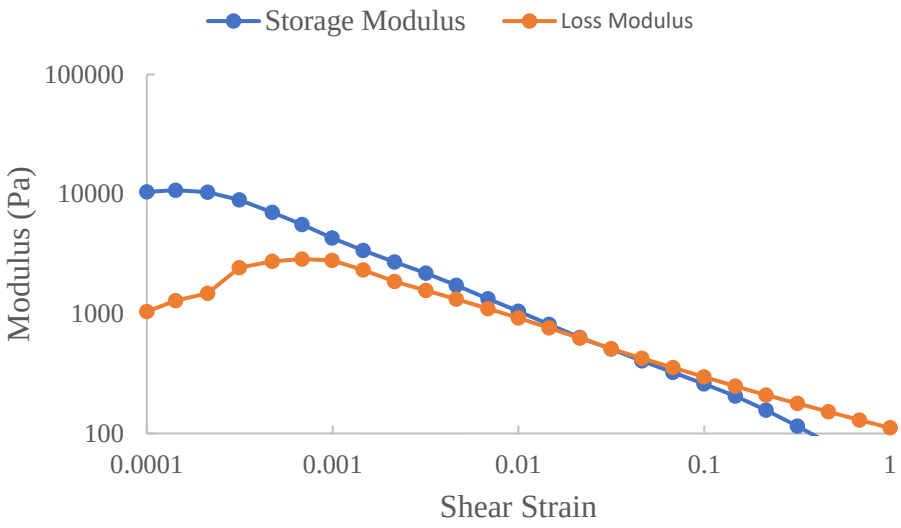

Figure 56: Storage and Loss Modulus vs Shear Strain for Sample 3 of the Carbon Nanotube Mixture

4.5: CFD

Using the results of the previously conducted rheological study, a computational fluid dynamics (CFD) study was conducted on the nozzle. The software chosen to carry this out was Ansys Fluent, using an Ansys Fluid Flow (Fluent) simulation. This was conducted using a student license, on the academic version of the software, acquired from the University of Oklahoma. The CFD simulation was only ran for the silicon rubber mixture and not the carbon nanotube mixture, as the carbon nanotube mixture was not printed using these nozzle designs.

To model the silicon rubber material, a constant viscosity liquid was input into Ansys, with the viscosity chosen based upon the rheological data. Since it is a shear-thinning fluid, the more shear that is applied, the lower the viscosity, and the easier it flows through the nozzle, behaving more like a liquid than a solid. According to Zheng et

al, during DIW, the wall of the nozzle experiences shear values ranging from approximately 1391 Pa to 4083 Pa [34]. While the actual values depend on a wide variety of factors, such as the material printed, printing pressure, nozzle material, and nozzle geometry, this can provide an initial starting point for determining the material viscosity. Selected viscosity values in Table 5 below were chosen from the range of the shear rate – viscosity curve correlating to these shear values reported by Zheng et al [34]. Based upon the shear stress values and viscosities shown in Table 5 below, a viscosity of 2500 mPa*s was chosen for CFD evaluation in Ansys, as this viscosity value was fairly accurate at all shear stress values reported by Zheng et al.

Table 5: Shear Rate, Shear Stresses, and Viscosities from the Three Tested Samples of Silicon Rubber Filament

Shear Rate (1/s)	Shear Stress (Pa)	Viscosity (mPa*s)
728	2125.6	2919.4
	2113.2	2902.9
	2154.4	2958.8
1090	2888.5	2648.1
	2902.4	2660.8
	2953.4	2707.8
1340	3353.7	2511.8
	3394.7	2542.9
	3433.5	2571.6
1630	3871.9	2369.2
	3927.6	2403.7
	3981.7	2436.8
2000	4429.3	2214
	4510.4	2255.1
	4540.1	2270.3

To import the geometry, a Step203 file was imported using the model generated. The two slots for the luer lock syringes were selected as inlets, with the nozzle tip selected as outlets, and the rest of the geometry to enclose this volume was selected as a wall. Figures 57-59 display this below. The outer surface of the nozzle was hidden to

only show the interior volume for analysis. Additionally, the nozzle was meshed with default settings, with a total of 5376 nodes and 23492 elements.

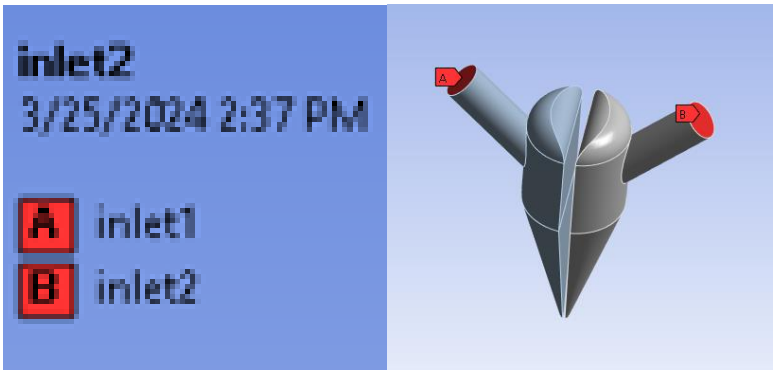

Figure 57: Inlets for CFD Analysis

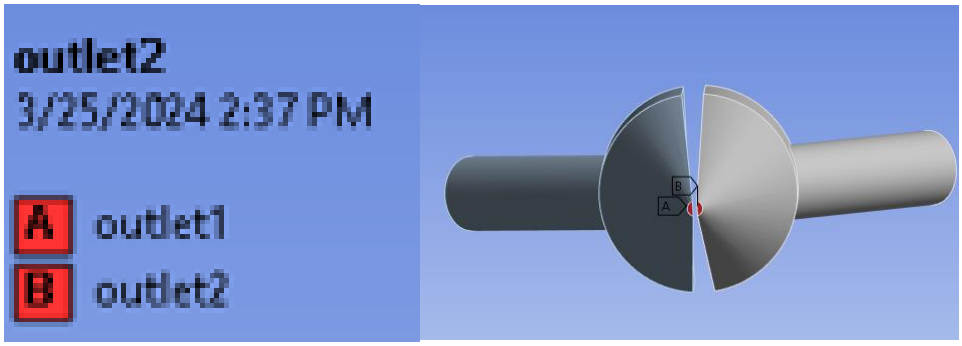

Figure 58: Outlets for CFD Analysis

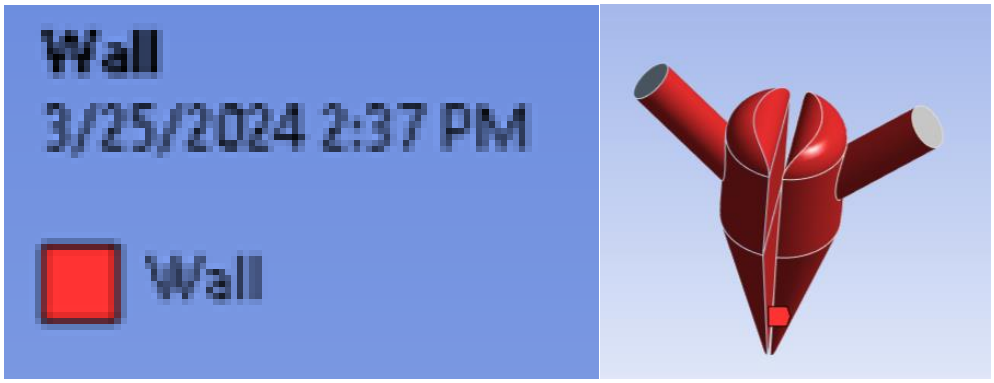

Figure 59: Wall Enclosing the Interior Volume for CFD Analysis

During the CFD analysis, all default values in Ansys Fluent were used unless otherwise specified. Material properties to simulate the material, using the viscosity found in the rheological study from Chapter 4.4 and the density of the material from the Smooth-On website are shown in Figure 60 below [11].

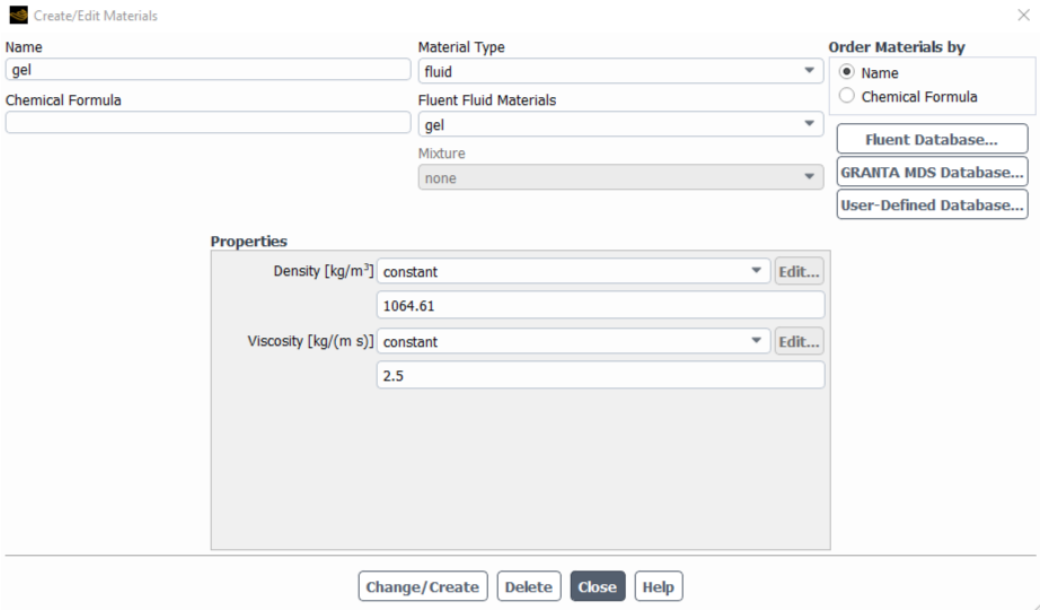

Figure 60: Material Properties to Simulate the Silicon Rubber Material in Ansys Fluent

Initial velocities at the inlet of the nozzle were calculated based upon the conservation of mass, with the equation given in Equation (2) below.

$$(2).\ \rho_1 V_1 A_1 = \rho_2 V_2 A_2$$

Where ρ is the density of the fluid, V is the velocity, and A is the area. Location 1 refers to the inlet of the nozzle, with location 2 referring to the outlet of the nozzle. Since the fluid that was moved through the nozzle was the same at both location 1 and location 2, with a negligible change in temperature since the fluid was printed at room temperature, $\rho_1 = \rho_2$. Both the inlet area and the outlet area are known and using the printing feed rate of 150 millimeters per second, the inlet velocity can be found for the idealized case. The inlet and outlet areas are 0.089727 square inches and 0.001924 square inches, respectively. Thus, an inlet velocity of 0.126646 inches per second, or 0.0032168084 meters per second. The inlet conditions are shown in Figure 61 below.

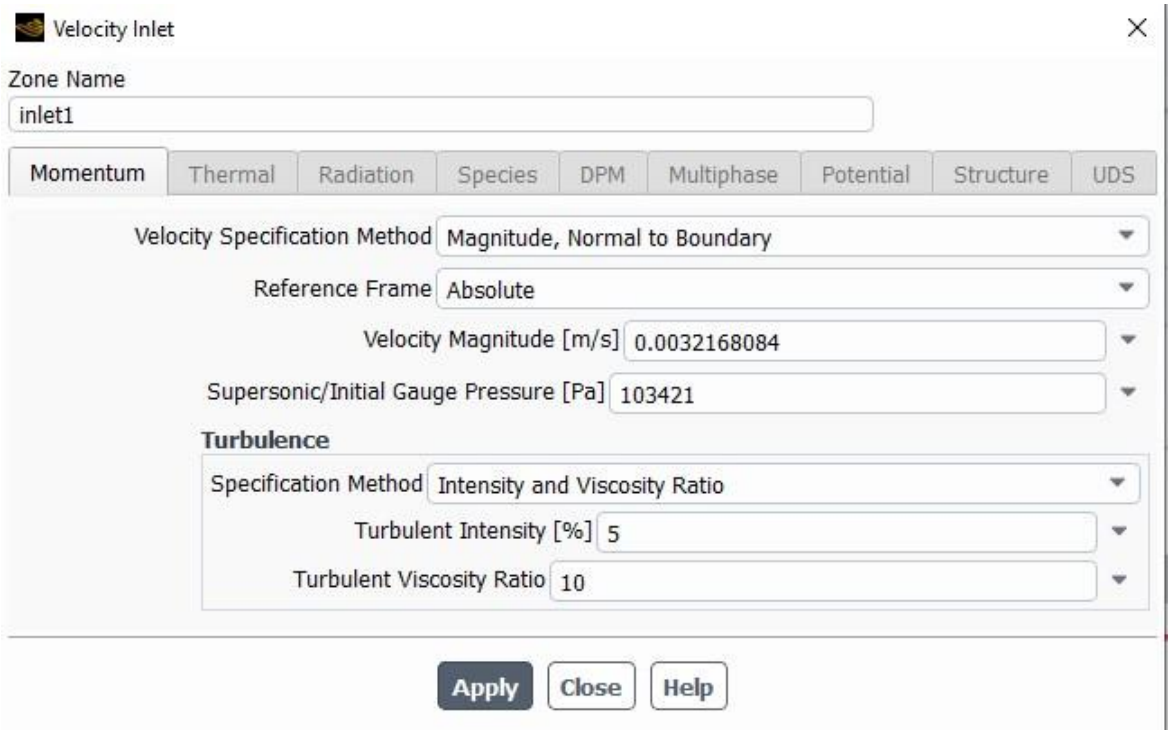

Figure 61: Inlet Conditions for CFD Analysis

200 iterations were used for CFD simulation. The results are shown in Figures 62 - 65 below.

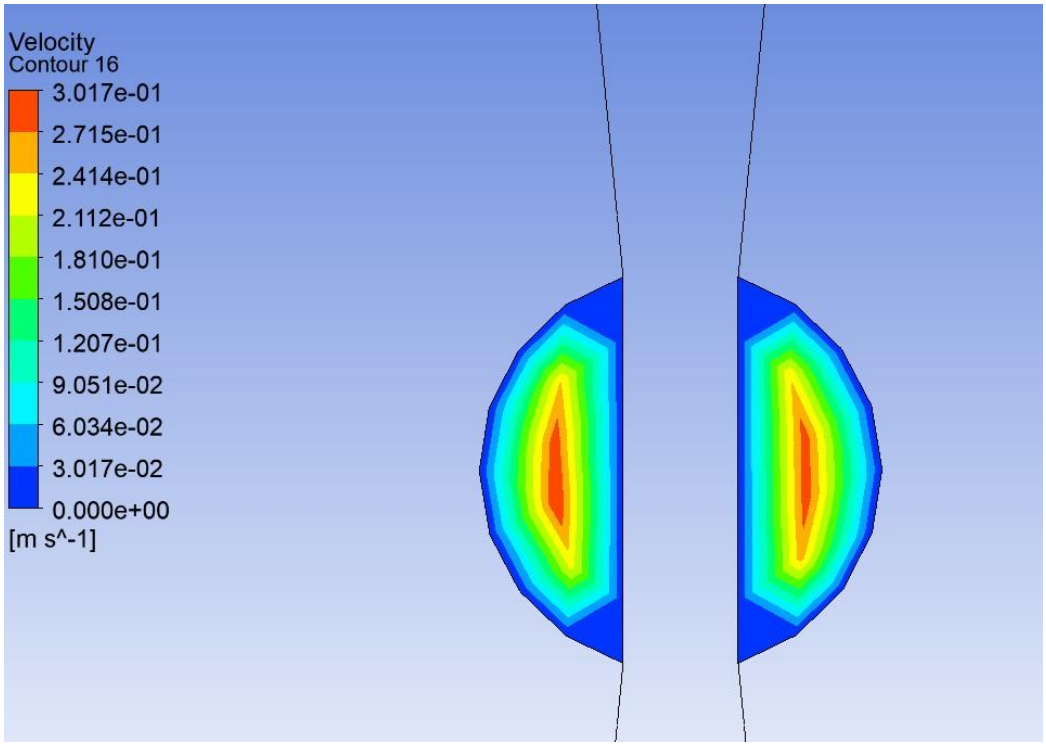

Figure 62: Outlet Velocities from CFD Analysis

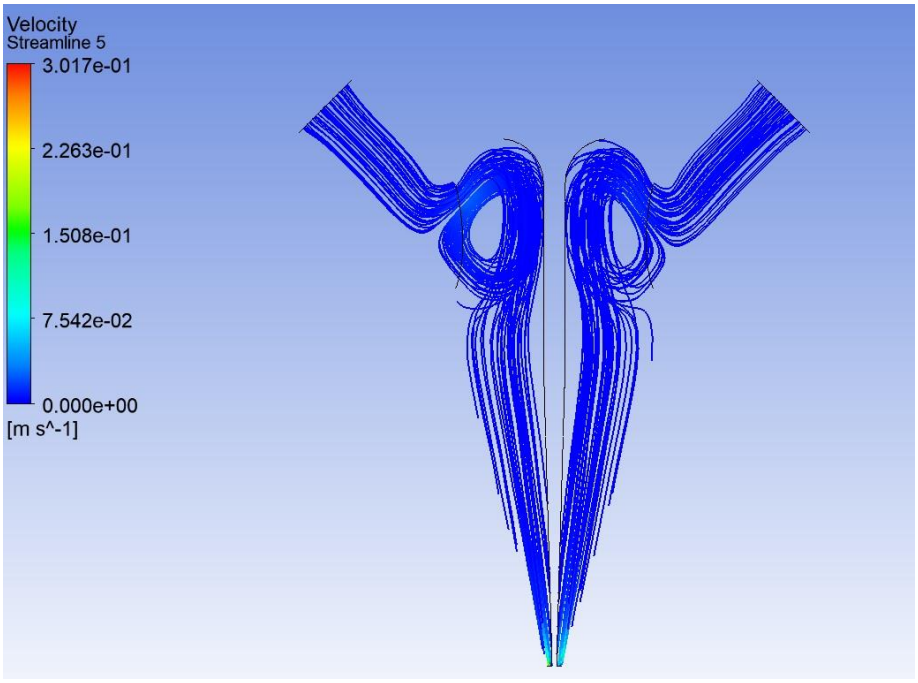

Figure 63: Streamlines from CFD Analysis

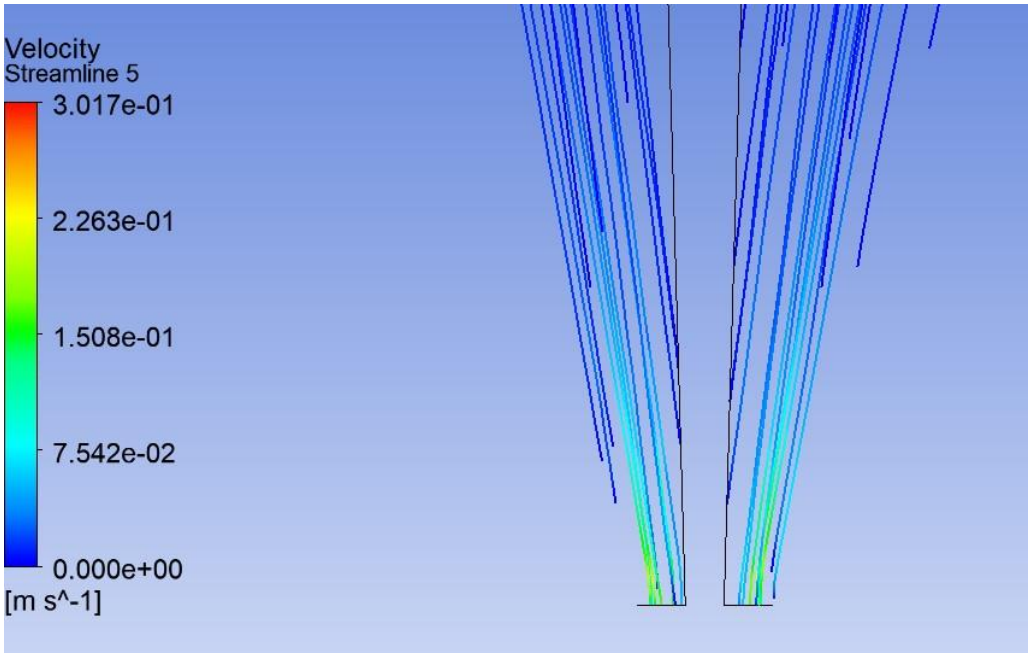

Figure 64: Zoomed in Streamlines from CFD Analysis

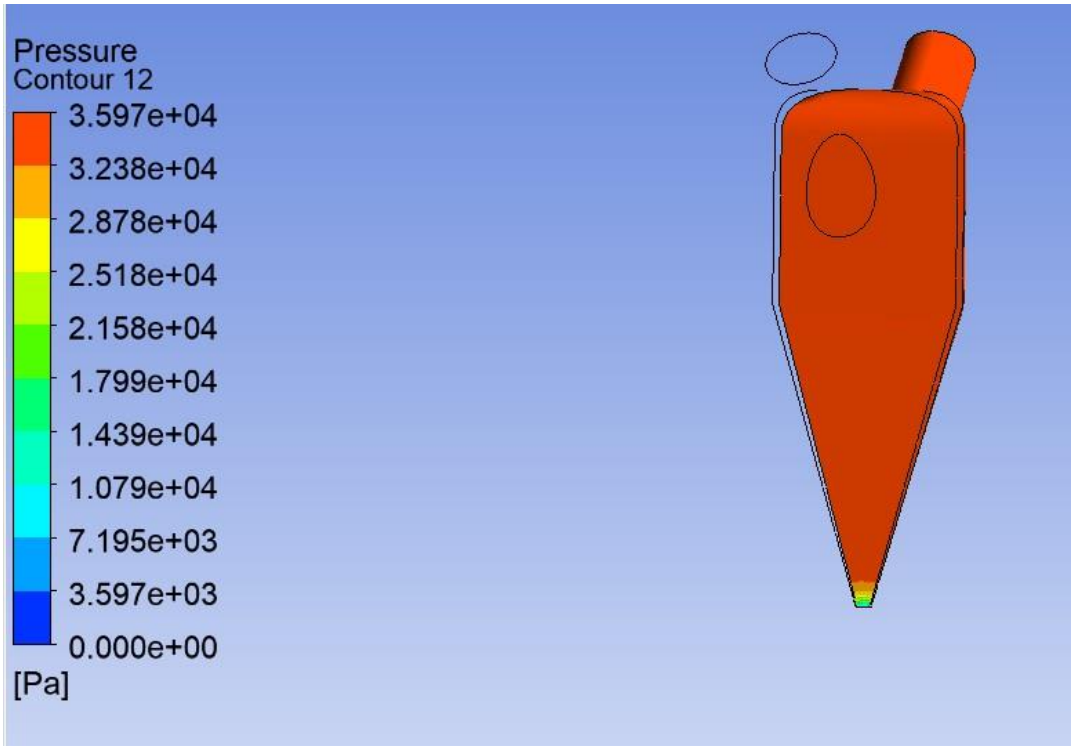

Figure 65: Interior Wall Pressures Found During CFD Analysis

In Figures 62 - 65 above, the CFD results are displayed. Outlet velocities are shown in Figure 62, with the highest velocities in the center of the nozzle outlet, with zero velocity at the wall. Additionally, wall velocities were viewed to confirm the no-slip boundary condition. The streamlines in Figures 63 and 64 show that fluid flows smoothly through the nozzle and to the tip, with Figure 64 showing that the velocities vastly increase in magnitude near the tip. The pressures shown in Figure 65 show the forces upon the wall of the nozzle as the filament is printed. These pressures were used in Chapter 3.5 to conduct a structural analysis of the nozzle, to ensure that the wall thickness was sufficient.

4.6: Geometric Measurements of Print Attempts

A study was also conducted to discover the best combination of values for printing pressure and printing speed that delivers the most accurate results. The printing pressures chosen were 5, 7.5, and 10 psi for both sides of the nozzle, with the chosen printing speeds being 100, 150, and 200 millimeters per second. Both sides of the nozzle experienced the exact same pressures. These values were selected based on previous experience printing the silicon rubber mixture through the multi-material nozzle. The minimum pressure required to extrude the material through the nozzle is approximately 5 psi; at lower pressures, material does not flow.

The silicon rubber mixture for the study was mixed in the exact same way described in Chapter 4.1 previously, to maintain consistency throughout all print attempts. All three print conditions for a specific pressure were printed using the same material, as all three G-codes only took approximately 1-2 minutes to run, with a new mixture created for each set of pressures. The outer diameter of the nozzle is 0.075

inches, or 1.9 millimeters. The desired diameter of the filament will be near the diameter of the nozzle while still laying down a filament with both green and purple filament easily visible. Diameter 1 refers to the diameter of the first line of filament printed, located closer to Y = 0 than the other line of filament. Consequently, diameter 2 refers to the second line of filament printed. The center point of the two lines in the G-code is exactly 20 millimeters apart, with the two lines being 110 millimeters long. This was measured by measuring the distance between the two lines at their two edges that are closest to each other, and then adding one half of the diameter of each line to that value. Ideally, the printed lines should be exactly 20 millimeters apart. The prints were allowed to cure for 24 hours following extrusion before being measured, with the measurement results described in Table 6 below. All measurements were recorded using a pair of digital, stainless hardened calipers.

Table 6: Measurements of Filament Diameters and Distances at Various Pressures and Feed Rates

Print Speed (mm/s)	Print Pressure (psi)	Diameter 1 (mm)	Diameter 2 (mm)	Distance between 2 lines (mm)
100	5	4.04	3.97	20.175
100	7.5	7.34	7.50	20.2
100	10	n/a	n/a	n/a
150	5	2.99	3.03	20.04
150	7.5	6.54	6.93	20.125
150	10	9.23	10.18	20.045
200	5	2.58	2.59	20.215
200	7.5	5.44	5.28	20.25
200	10	7.57	8.21	19.95

Figure 66 below shows an example of the geometry of the print, with the lines being 20 millimeters apart and 110 millimeters long. The print conditions for Figure 66 were at a feed rate of 150 millimeters per second and a pressure of 7.5 psi.

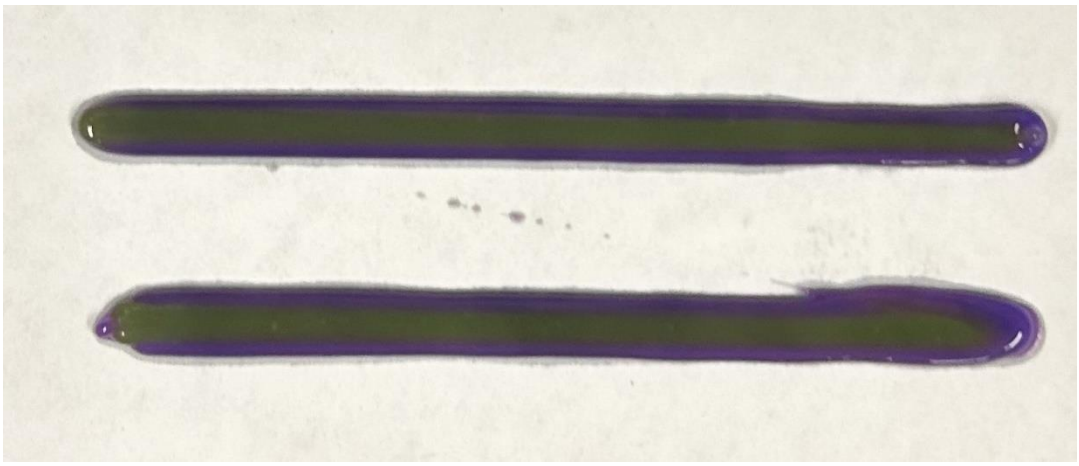

Figure 66: Example of the Print Geometry at 150 millimeters per second and 7.5 psi

Figure 67 below shows the image of the print when the pressure was 10 psi and the printing speed was 100 mm/s. As this was the highest pressure and the lowest feed rate, it was the condition in this study that resulted in the most material being deposited per unit of print distance. Accurate measurements for this sample were unable to be taken, as can be seen in Figure 67. The diameter of the line grew as the print went on, likely due to significantly less mass of filament being in the syringe to resist the 10 psi of pressure applied, with this effect compounding as less and less material was in the syringe. This also caused the distance between the two lines to be difficult to measure, as at the end of the print, they end up touching. This effect with the increasing diameter of the filament as the print goes on was seen in other conditions for this study, although not to as the same extreme as the 100 mm/s and 10 psi print condition. To a lesser extent, it was also seen in all conditions with print lines thicker than 6 millimeters. The second line printed had a thicker diameter, by up to 0.5 millimeters. This is likely due to as the material is extruded, less material is remaining in the syringe to resist the pressure, so this results in the extrusion of more material. The fluid is more affected by

shear forces applied during printing, as there is less fluid remaining in the syringe, resulting in a lower viscosity of the material, and more material being extruded during printing. Additionally, this could be due to less surface area from the filament on the sides of the syringe, resulting in less frictional forces, making extrusion easier. When the print has a diameter around 4 millimeters or less, this effect is more negligible due to the amount of material in the syringe. This also shows that these conditions described deposit far too much material to be ideal to print with.

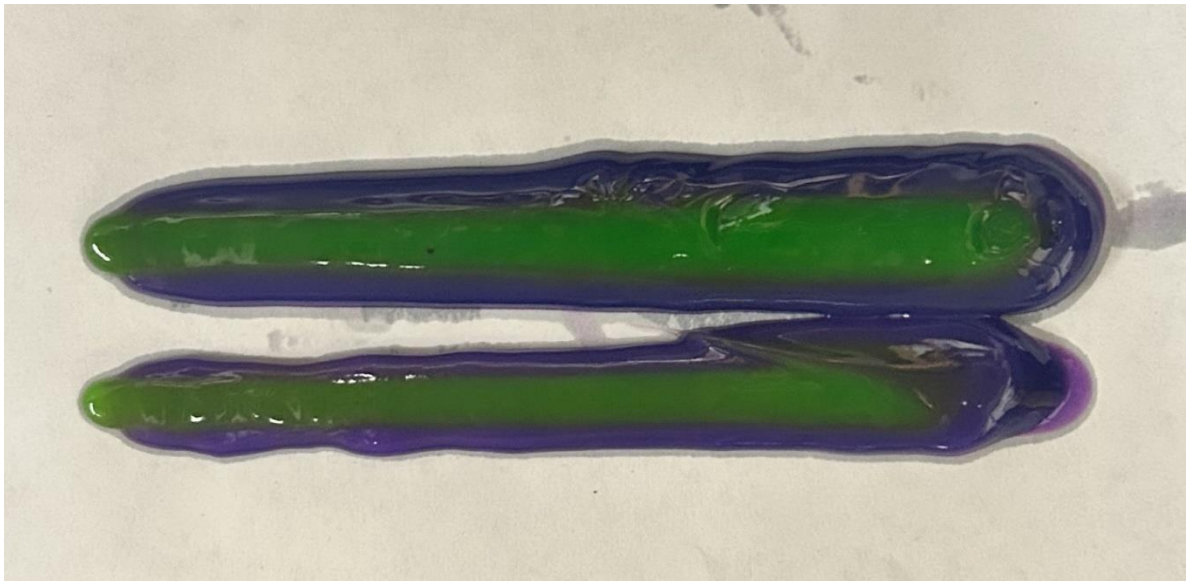

Figure 67: Print Results for the 10 psi and 100 mm/s Condition

Based upon the above results, the two printing conditions that work best for the designed nozzle size are 150 mm/s and 5 psi, and 200 mm/s and 5 psi. Closeup images of both print conditions are shown below in Figures 68 and 69. For print attempts, 150 mm/s and 5 psi were chosen because despite leaving a slightly thicker print filament line than 200 mm/s and 5 psi, it is far easier to see both colors of filament. This is important during initial print attempts to ensure visually that both sides of the nozzle are

extruding filament as intended, to make troubleshooting issues easier. Following initial tests of the nozzle, 200 mm/s and 5 psi is a better printing condition as it is closer in diameter to the diameter of the nozzle. The 20-millimeter distance between the lines served as both a check on the caliper measurement accuracy as well as a check on the accuracy of the modified Ender 3 coordinate accuracy.

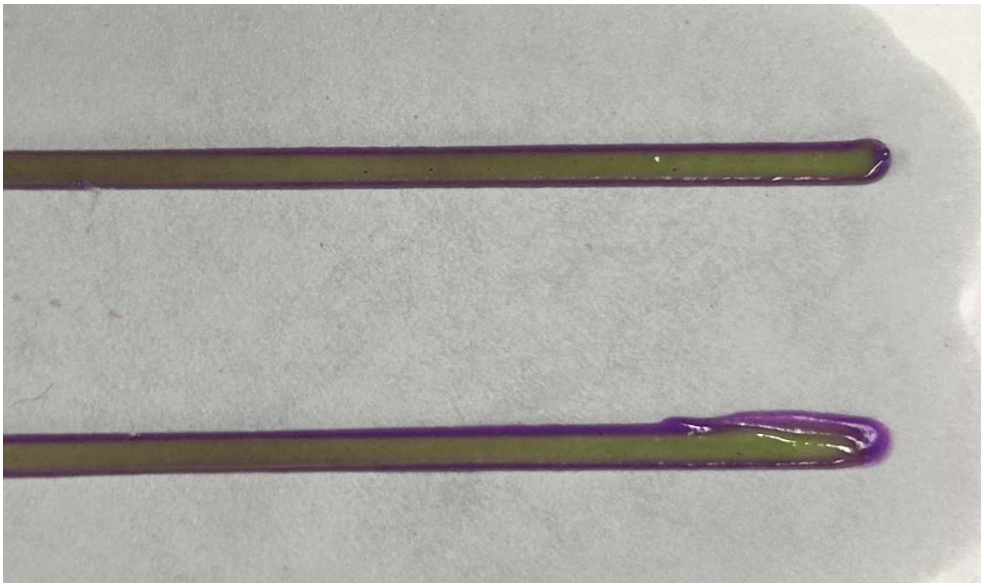

Figure 68: Closeup Image of 150 mm/s and 5 psi Print Condition

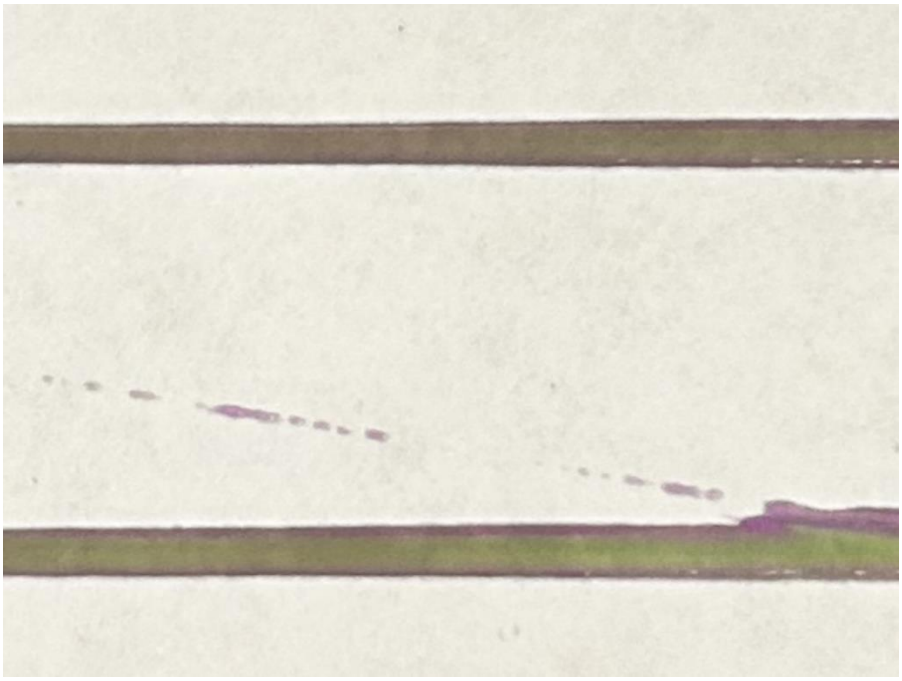

Figure 69: Closeup Image of 200 mm/s and 5 psi Print Condition

Chapter 5: Conclusions and Future Work

5.1: Conclusions

The nozzle design that was manufactured, tested, and analyzed, was capable of printing multiple materials at once, provided the printing material has a high enough viscosity along with shear-thinning properties. Complex two-dimensional geometries were successfully demonstrated and analyzed using this printing method, with print times approaching 10 minutes with zero pressure adjustments throughout the duration of the print. Additionally, the nozzles were capable of being manufactured cheaply, allowing for disposable usage with little financial impact. Using the modified Ender 3 printer at the University of Oklahoma, multi-material direct ink writing material extrusion was proven to be capable of creating desired geometry.

5.2: Future Work/Recommendations

The nozzle designs for 2 materials were the only ones tested out of all the nozzle designs, as there are only two pneumatic connections on the modified Ender 3 used for print attempts. Only the two-material circular nozzle was tested to simplify the testing regime of the nozzles. All the nozzles designed were capable of being manufactured in the same method that the tested two material nozzle was, so if more pneumatic connections existed or were added on the printer, more nozzle designs could be tested and analyzed.

Only one material was tested using the nozzles. The left and right side of the two-material circular nozzle both had the same type of material in them throughout all tests conducted. This simplified the testing regime, ensuring that the pressure of both sides of the nozzle was roughly equivalent and the materials on both the left and right side

behaved in a similar manner. However, additional testing should be necessary using two different materials on either side of the nozzle to observe the printing capabilities with two different materials. It should still perform very similarly to the previous tests conducted, as the materials are kept separated up until the tip of the nozzle.

Additionally, three-dimensional geometry was never tested out using the designed nozzles, either free floating or within a resin bath. The only geometry that was printed was two-dimensional geometry, with the most complex design tested being the University of Oklahoma logo. Using either a resin bath, or a different material, three-dimensional geometry should be tested with the nozzle designs.

Vacuum pressure for the pneumatic connections would also be very helpful to withdraw the material back into the nozzle once printing is complete. Throughout printing tests, material leaking out of the nozzle when not desired was a common issue. As more THI-VEX was added to the material formula, this helped mitigate the issue, however, it still existed. Additionally, when printing the two squares side by side using the multi-material nozzles, sometimes after printing the first square, when a bit of extra material would leak out of the nozzle, it would need to be wiped off. This would then cover up the exit of the nozzle, clogging the nozzle, and ruining the next print. Vacuum pressure would help mitigate and hopefully fix this issue.

Another future improvement that could be made to the nozzle is to allow it to rotate, depending on the side-by-side alignment of the material desired. Currently, the nozzle does not rotate as the print goes, with the green filament always on the left side of the print and the purple filament always on the right side of the print. Consequently, as the print goes in the positive X direction, the green filament always ends up on top of

the purple filament, and in the negative X direction, the purple filament is on top. In both the positive and negative Y direction, the green filament is side-by-side on the left side of the purple filament. This could be improved as geometry is created parallel to the X direction.

Additionally, the interior volume of the nozzle could be optimized to waste less printing filament, with a smaller volume. This could run into issues with manufacturing though, as a smaller interior volume would have smaller dimensions and tighter tolerances to hit, some of which may not be capable on a Photon Mono M5s resin printer. Optimization of the interior volume, where the size of the hole on the nozzle is reduced from the connection on the 10cc syringe barrel to the tip of the nozzle, could waste less filament.

Reuse of the nozzles was also explored in Chapter 4.1, although ultimately a one-time use method was decided upon. If a method was found to reuse the nozzles by cleaning out the inside of the nozzle without contaminating future prints, this would be ideal as a new nozzle would not have to be printed for every print attempt.

References

1. Patel, S., et al., *A review of wearable sensors and systems with application in rehabilitation*. Journal of neuroengineering and rehabilitation, 2012. **9**: p. 1-17.
2. Kristoffersson, A. and M. Lindén, *A systematic review of wearable sensors for monitoring physical activity*. Sensors, 2022. **22**(2): p. 573.
3. Abshirini, M., et al., *3D printing of highly stretchable strain sensors based on carbon nanotube nanocomposites*. Advanced Engineering Materials, 2018. **20**(10): p. 1800425.
4. Homayounfar, S.Z. and T.L. Andrew, *Wearable sensors for monitoring human motion: a review on mechanisms, materials, and challenges*. SLAS TECHNOLOGY: Translating Life Sciences Innovation, 2020. **25**(1): p. 9-24.
5. Lou, Z., et al., *Reviews of wearable healthcare systems: Materials, devices and system integration*. Materials Science and Engineering: R: Reports, 2020. **140**: p. 100523.
6. Chowdhury, S.A., et al., *Highly conductive polydimethylsiloxane/carbon nanofiber composites for flexible sensor applications*. Advanced Materials Technologies, 2019. **4**(1): p. 1800398.
7. Abshirini, M., et al., *Functional nanocomposites for 3D printing of stretchable and wearable sensors*. Applied Nanoscience, 2019. **9**: p. 2071-2083.
8. Charara, M., et al., *Investigation of lightweight and flexible carbon nanofiber/poly dimethylsiloxane nanocomposite sponge for piezoresistive sensor application*. Advanced Engineering Materials, 2019. **21**(5): p. 1801068.
9. Segev-Bar, M. and H. Haick, *Flexible sensors based on nanoparticles*. ACS nano, 2013. **7**(10): p. 8366-8378.
10. Mamun, M.A.A. and M.R. Yuce, *Recent progress in nanomaterial enabled chemical sensors for wearable environmental monitoring applications*. Advanced Functional Materials, 2020. **30**(51): p. 2005703.
11. Smooth-On. *Ecoflex Series Technical Bulletin*.
12. Herren, B., et al., *Development of ultrastretchable and skin attachable nanocomposites for human motion monitoring via embedded 3D printing*. Composites Part B: Engineering, 2020. **200**: p. 108224.
13. Zhang, J., et al., *A high anti-impact STF/Ecoflex composite structure with a sensing capacity for wearable design*. Composites Part B: Engineering, 2022. **233**: p. 109656.
14. Liao, Z., et al., *The time and temperature dependences of the stress recovery of Ecoflex polymer*. International Journal of Non-Linear Mechanics, 2023. **149**: p. 104338.
15. Plastics, M. *Thermoset vs. Thermoplastics*.
16. Matsuda, R., et al., *Highly stretchable and sensitive silicone composites with positive piezoconductivity using nickel powder and ionic liquid*. APL Bioeng, 2023. **7**(1): p. 016108.
17. Cholleti, E.R., et al., *Highly Stretchable Capacitive Sensor with Printed Carbon Black Electrodes on Barium Titanate Elastomer Composite*. Sensors, 2019. **19**(1): p. 42.

18. Beaman, J.J., et al., *Additive Manufacturing Review: Early Past to Current Practice*. Journal of Manufacturing Science and Engineering, 2020. **142**(11).
19. Tofail, S.A.M., et al., *Additive manufacturing: scientific and technological challenges, market uptake and opportunities*. Materials Today, 2018. **21**(1): p. 22-37.
20. Saadi, M.A.S.R., et al., *Direct Ink Writing: A 3D Printing Technology for Diverse Materials*. Advanced Materials, 2022. **34**(28): p. 2108855.
21. Skylar-Scott, M., et al., *Voxelated soft matter via multimaterial multinozzle 3D printing*. Nature, 2019. **575**: p. 330-335.
22. Xu, C., et al., *Multi-Material Direct Ink Writing (DIW) for Complex 3D Metallic Structures with Removable Supports*. ACS Applied Materials & Interfaces, 2019. **11**(8): p. 8499-8506.
23. Uzel, S.G.M., et al., *Multimaterial Multinozzle Adaptive 3D Printing of Soft Materials*. Advanced Materials Technologies, 2022. **7**(8): p. 2101710.
24. Muth, J.T., et al., *Embedded 3D Printing of Strain Sensors within Highly Stretchable Elastomers*. Advanced Materials, 2014. **26**(36): p. 6307-6312.
25. Tech, S., *Siraya Tech Build-Drillable Precision Printing Resin*.
26. Tech, S. *Siraya Tech Technical Data Sheet*.
27. Chen, D.T.N., et al., *Rheology of Soft Materials*. Annual Review of Condensed Matter Physics, 2010. **1**(Volume 1, 2010): p. 301-322.
28. Mezger, T.G., *Applied Rheology*. 2014: Anton Paar.
29. Bom, S., et al., *On the progress of hydrogel-based 3D printing: Correlating rheological properties with printing behaviour*. International Journal of Pharmaceutics, 2022. **615**: p. 121506.
30. Liu, Z., et al., *Linking rheology and printability of a multicomponent gel system of carrageenan-xanthan-starch in extrusion based additive manufacturing*. Food Hydrocolloids, 2019. **87**: p. 413-424.
31. Barrulas, R.V. and M.C. Corvo, *Rheology in Product Development: An Insight into 3D Printing of Hydrogels and Aerogels*. Gels, 2023. **9**(12).
32. Herrada-Manchón, H., M.A. Fernández, and E. Aguilar, *Essential Guide to Hydrogel Rheology in Extrusion 3D Printing: How to Measure It and Why It Matters?* Gels, 2023. **9**(7): p. 517.
33. Than, Y.M., S. Suriyarak, and V. Titapiwatanakun, *Rheological Investigation of Hydroxypropyl Cellulose–Based Filaments for Material Extrusion 3D Printing*. Polymers, 2022. **14**(6): p. 1108.
34. Qingyang Zheng, B.X., Zhoulong Xu, Hao Wu, *A systematic printability study of direct ink writing towards high-resolution rapid manufacturing*. International Journal of Extreme Manufacturing, 2023. **5**(3).